Convergent evolution of sex chromosomes in two palm species, *Phoenix dactylifera* and *Kerriodoxa elegans*.

H. Tessarotto[1], T. Beulé[1], E. Cherif[1], J. Orjuela[1], P. Farhat[1], A. Lindström[2], A. Lemansour[3], S. Santoni[4], J. Käfer[5*], F. Aberlenc[1*]

[1] DIADE, Université de Montpellier, IRD, CIRAD; Montpellier, France.

[2] Global Biodiversity Conservancy, Thailand.

[3] United Arab Emirates University, UAE.

[4] AGAP, Université Montpellier, CIRAD, INRAe, Montpellier SupAgro; Montpellier, France.

[5] ISEM, Université Montpellier, CNRS, IRD; Montpellier, France.

***** *These authors contributed equally to this work.*

For correspondence: frederique.aberlenc@ird.fr jos.kafer@cnrs.fr

Summary

- In palms, many dioecious species have emerged from at least 8 independent events, yet the mechanisms of sex determination remain poorly understood. Here, we identify and compare the sex chromosomes of *Kerriodoxa elegans* with those of the well-studied date palm (*Phoenix dactylifera*), which evolved dioecy independently from a hermaphroditic common ancestor.
- We developed target sequence capture kits and inferred sex-linked genes using a probabilistic approach in both species.
- We find a striking similarity between the sex-linked regions of *K. elegans* and *P. dactylifera*, with the majority of sex-linked genes being common between the two species. However, we confirm that these regions evolved independently, much later than the split between the lineages.
- This case of convergent evolution seems to be unique in plants so far, and raises questions on the mechanisms of sex determination. A possible explanation is that this region contains genes related to flower sexual development, and is syntenic in monoecious palm species as well, suggesting it might serve as a genetic 'toolbox' for flower unisexualization in palms.

Keywords : Recombination arrest, date palm, Arecaceae, unisexuality, dioecy, sex determination

Introduction (1,068 words), Material and Methods (2,376 words), Results (2,324 words), Discussion (1,927 words) ~ 7,695 words

4 Figures, 1 Table, 1 supplementary notes, 9 supplementary tables, 9 supplementary figures, 6 supplementary files. All figures with color.

Introduction

Flowering plants are characterized by a large diversity in sexual systems. While most species have bisexual flowers (the presumed ancestral state, Sauquet *et al.*, 2017), unisexual flowers evolved rather frequently in many different clades. About 10% of species have unisexual flowers (Renner, 2014), either with flowers of both sexes on one plant (monoecy) or on different individuals (dioecy). Of about 15,000 dioecious angiosperm species, sex determination is only known in fewer than 100, distributed in about 30 genera (Leite Montalvão *et al.*, 2021; Charlesworth D & Harkess A, 2024). In most of these species, sex chromosomes are XY (male heterogamety), with small non-recombining regions, although there are some notable exceptions (Renner & Müller, 2021).

Sex chromosomes evolve from a pair of autosomes and once they have stopped recombining, the sex-limited chromosome (Y in XY systems) degenerates. This has dramatic consequences: deleterious mutations accumulate and many genes cease to function and can be lost (Ming *et al.*, 2011). However, what causes the initial recombination suppression and subsequent extensions of this region, leading to striking dissimilarities among species, remains poorly understood (Renner & Müller, 2021). In plants, sex-determining genes probably evolved independently with each transition to unisexuality, implying that they must be identified from scratch in each clade, and so far only a few such genes have been characterized (Henry *et al.*, 2018; Leite Montalvão *et al.*, 2021; Renner & Müller, 2021). How sex-determining genes might give rise to the initiation and extension of non-recombining regions typical of sex chromosomes remains an open question (Charlesworth & Charlesworth, 1978; Ponnikas *et al.*, 2018; Renner & Müller, 2021). Recent modeling studies have identified new possible mechanisms (Jeffries *et al.*, 2021; Lenormand & Roze, 2022; Jay *et al.*, 2022) but their predictions remain to be tested (Käfer, 2022).

The study of plants, and their repeated evolution of dioecy and sex chromosomes, could shed light on the generality of the evolutionary patterns and the processes behind them. In a few groups, comparative analyses of related species have been performed, yielding different results in each case. For example, in the genus *Silene*, that contains the model species *S. latifolia*, dioecy evolved independently in at least

three groups (Marais *et al.*, 2011). In two of these, species with sex chromosomes have been identified, with one group consisting of five species that share an ancestral well-differentiated sex chromosome pair, while in the other group sex-linked regions are small and likely to have undergone turnovers (Balounova *et al.*, 2019). In the Salicaceae family, dioecy is ancestral but different sex chromosome pairs have been found in different species, once again suggesting sex chromosome turnover (Hu N *et al.*, 2023). The two sister genera *Cannabis* and *Humulus* inherited a homologous sex chromosome system from their common ancestor with subsequent expansion of the non-recombining region in both, thus leading to a rather unique situation in plants during which quite degenerated sex chromosomes with a large non-recombining region have remained stable for more than 20 million years (Prentout *et al.*, 2021). The reasons for these differences are not understood.

Arecaceae (palms) are a large family of flowering plants with about 2,600 species (‘PALMweb’, 2025). It has a high proportion of species with unisexual flowers, with 52% being monoecious and 30% dioecious, as well as many transitions between these sexual systems. Consequently, it has been called “a microcosm of sexual system evolution” (Nadot *et al.*, 2016). Ancestral state reconstructions do not provide a consensus on whether the common ancestor of all palms exhibited monoecy or hermaphroditism, but it is clear that dioecy has evolved independently in several palm clades (Figure 1; Nadot *et al.*, 2016; Cássia-Silva *et al.*, 2021).

Sex chromosomes are known to occur in the date palm *Phoenix dactylifera* (Siljak-Yakovlev *et al.*, 1996; Cherif *et al.*, 2013; Mathew *et al.*, 2014), and are shared across its genus (Cherif *et al.*, 2016; Torres *et al.*, 2018). Despite their relatively old age compared to other dioecious species with sex chromosomes (Renner & Müller, 2021), their non-recombining region has remained small, and the chromosomes have not evolved into a distinctly heteromorphic pair. Torres *et al.* (2018) identified two genes involved in male organ development absent from the X chromosomes, along with another gene that could inhibit female organ development. They suggested that this scenario fits the “two linked sterility mutations” model (Charlesworth & Charlesworth, 1978), with dioecy evolving through a gynodioecious intermediate. However, gynodioecy is absent or very rare in palms (Nadot *et al.*, 2016), and the function of the identified genes has not been demonstrated in date palm. Evidence for genetic sex determination has also been found in *Trachycarpus fortunei*, where its XY chromosome system seems to be quite young and unstable (Jousson *et al.*, 2023), and possibly in *Lodoicea maldivica* (Morgan *et al.*, 2020).

Here we focus on the dioecious species *Kerriodoxa elegans*, for which sex chromosomes have not been previously described, and compare its sex determination with that of the date palm. *K. elegans* is the only species of its genus and was discovered rather recently in Phuket island in Thailand (Dransfield, 1983). According to ancestral state reconstructions, *K. elegans* evolved dioecy independently from the genus *Phoenix*, most probably from a hermaphroditic ancestor (Figure **1**; Nadot *et al.*, 2016; Cássia-Silva *et al.*, 2021). For comparative analyses on the scale of the palm family, we developed two sequence capture kits targeting exons genome-wide as well as known sex-linked genes, applicable across the palm family. As coding sequences are relatively well conserved among distantly related species (Heyduk *et al.*, 2016; Comer *et al.*, 2016), this approach allows the direct comparison of sex-linked genes, their evolution and hypothetical function (cf Prentout *et al.*, 2021). Sex-linkage was identified through the probabilistic approach SDpop, which is based on the detection of genotype frequencies typical of recombination suppression (Käfer *et al.*, 2021) and has been successfully applied to long-lived species that cannot be easily bred in the lab (e.g. *Amborella*, Käfer *et al.*, 2022). This approach also allows reconstructing the consensus sequences of the X and Y copies of the sex-linked genes, which were subsequently used for phylogenetic analysis of these genes. We tested these tools on the known sex chromosomes of *P. dactylifera* before applying them to *K. elegans*. We then showed that *K. elegans* has a XY sex determination system that evolved independently from the one in *P. dactylifera*, but has striking similarities that raise intriguing questions about the evolution of sexual systems in palms.

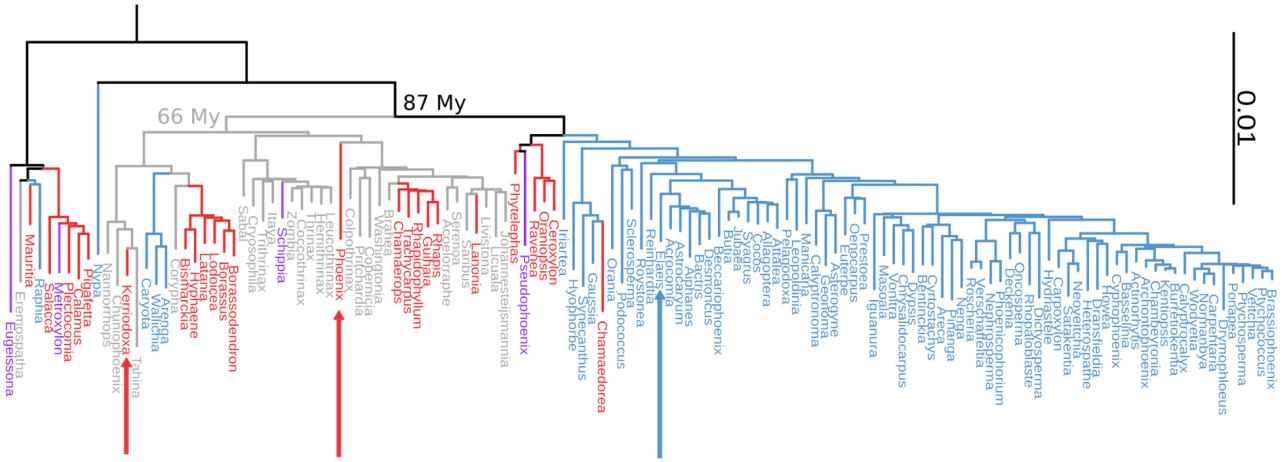

Figure 1 : Representation of the sexual system diversity within the palm family in a phylogenetic framework. The plastid phylogeny of palms from Yao *et al.* (2023) is colored according to the sexual system, as classified by Nadot *et al.* (2016) and Cássia-Silva *et al.* (2021): monoecy (blue), dioecy (red), hermaphroditism (grey), and polygamy (purple). Black branches indicate inconclusive ancestral state reconstruction. The branch length corresponds to the number of the estimated substitutions per base (Yao *et al.*, 2023). The estimates of the age of the hermaphroditic most recent common ancestor (MRCA) of *Phoenix dactylifera* and *Kerriodoxa elegans* as well as their MRCA with *Elaeis guineensis* (unresolved sexual system, either hermaphroditic or monoecious) are based on Baker & Couvreur (2011). The *Phoenix* and *Kerriodoxa* genera are indicated by red arrows and *Elaeis* genus by a blue arrow.

Material & Methods

Plant material and DNA extraction

Leaf samples of 10 females and 10 males of *P. dactylifera* were collected in Al Ain, United Arab Emirates and 14 females and 11 males of *K. elegans* in Puerto Rico (Central Cordillera) and in Thailand (Nong Nooch Tropical Botanical Garden). DNA was extracted from 15 mg of dried leaves with the Chemagic DNA Plant Kit (Perkin Elmer Chemagen, Baesweller, DE, Part # CMG-194), according to the manufacturer's instructions. The protocol was adapted to the use of the KingFisher Flex™ (Thermo Fisher Scientific, Waltham, MA, USA) automated DNA purification workstation.

Targets and baits design

We designed two separate sets of capture targets. The first one, SexPhoenix (SP), was developed to focus primarily on sex-determining regions. This set includes potential sex-linked genes of *P. dactylifera* (Al-Dous *et al.*, 2011; Cherif *et al.*, 2016; Torres *et al.*, 2018). To enable comparative analysis with these genes, we added nuclear genes unrelated to sex (e.g. salt tolerance genes), chloroplast genes (e.g. *pbsZ* and *trnG),* and highly conserved low-copy protein-coding nuclear and plastid genes from Heyduk *et al.* (2016). In total, SexPhoenix target set comprises 920 regions (File **S1**). To identify additional potentially sex-linked genes not previously characterized, we developed PalmExon (PE) set, using the transcriptomic data of *P. dactylifera* (NCBI Bioproject PRJNA83433). This target set captures two exonic regions of 30,000 protein-coding nuclear genes (File **S2)**.

From the SexPhoenix and PalmExon target sets, 38,884 and 60,000 enrichment baits were designed, respectively, with a 30-base overlap between baits in SexPhoenix. These consist of biotinylated RNA probes of 90-mers (SexPhoenix) and 80-mers (PalmExon) synthesized by MYcroarray (Arbor Biosciences, MI, USA).

Target enrichment

For each sample, 100 ng of total DNA were shredded using the NEBNext Ultra II FS DNA Modul (New England Biolabs, Ipswich, MA, USA). The fragmented DNA was ligated to the adapters and the genomic library was constructed following published protocols (Rohland & Reich, 2012; Mascher *et al.*, 2013) with some modifications. Two hybridization reactions were implemented, one for each bait kit. In each hybridization reaction, a maximum of 24 samples were multiplexed into one pool, giving a

total of 2 pools per reaction. All hybridization steps followed the myBaits protocol version 4.01 (http://www.mycroarray.com).
The final pooled library was sequenced using the Illumina paired-end protocol (2x150bp) on HiSeq3000 sequencer (Novogene, Beijing, China). The detailed protocol for sequence capture is presented in the Supplementary notes.

Mapping and genotyping

For comparison with the capture kits, we downloaded whole genome sequencing (WGS) data of 20 female accessions and 12 male accessions of *P. dactylifera* from NCBI (bioproject PRJNA505141, Hazzouri *et al.*, 2019). In total we analyze five different datasets: (i) WGS *P. dactylifera*, (ii) PalmExons (PE) *P. dactylifera*, (iii) SexPhoenix (SP) *P. dactylifera*, (iv) PalmExons (PE) *K. elegans* and (v) SexPhoenix (SP) *K. elegans*. We used 4 genome assemblies for our analysis, 2 of which from *P. dactylifera* : the homogametic (XX) female DPV01 (Al-Mssallem *et al.*, 2013) and heterogametic (XY) male PDMBC4 (Hazzouri *et al.*, 2019). The last two are from *Elaeis guineensis* (oil palm), the EG5 (Singh *et al.*, 2013) and EGPMv6 (Ong *et al.*, 2020) genomes. EGPMv6 is the only one not annotated.

A visual summary of the detection and study of sex-linked sequences is presented in Figure **S1**. For the detection of XY polymorphisms, we used the female (XX) DPV01 genome of *P. dactylifera* as a reference for mapping. In addition to the fact that XY polymorphisms can be detected more reliably than X- or Y-hemizygosity (Käfer *et al.*, 2021), assembled genomes from the heterogametic sex might be partially chimeric in the non-recombining region due to the known difficulties of assembling them (Tomaszkiewicz M *et al.*, 2017; cf Käfer *et al.*, 2021), making the inference of the gametologous haplotypes more difficult. We used the BWA mem2 algorithm (version 2.2.1; Li & Durbin, 2009; Vasimuddin *et al.*, 2019) to map the reads, lowering the penalty for mismatches from 4 to 2 (option -B 2), to allow more divergent reads (Y chromosome, *K. elegans*) to be correctly mapped. For comparison with the most recent chromosome-level assembly (PDMBC4) we identified the position of DPV01 annotation with Liftoff (Shumate & Salzberg, 2021). *E. guineensis* assemblies were used to compare synteny and gene content between genomic regions. The unannotated EGPMv6, was used for synteny analyses, while the EG5 annotation was used to identify the homologous genes between *P. dactylifera* and *E. guineensis*. Liftoff was used to position the *E. guineensis* EG5 and *P. dactylifera* DPV01

annotated genes on the *E. guineensis* EGPMv6 assembly (Ong *et al.*, 2020). Y-specific genes not present on the DPV01 assembly were studied by recovering unmapped reads and aligning them on the PDMBC4 assembly.

Coverage depth for each base was calculated using bedtools 2.30 genomecov (Quinlan & Hall, 2010). We calculated the mean depth for 100 base windows for all samples, as well as the average for each sex. To calculate the mean depth per gene, we used the windows with at least 50% overlap with genes CDS. To calculate the proportion of female reads for each 100 base windows, we accounted for possible read depth differences between samples by normalizing the depth of each individual. To do so, for each window, the mean depth was divided by the median of the mean depth of all windows of each individual.

SNP calling was done with bcftools mpileup (version 1.9; Danecek *et al.*, 2011; Lefouili & Nam, 2022). Genotypes with fewer than 7 reads for the capture data and 10 for the WGS data were discarded. The resulting vcf file was then filtered to keep only the sites within coding sequences according to the DPV01 annotation. We conducted a Principal Component Analysis (PCA) of the genetic variation between individuals using plink 1.90 (Purcell *et al.*, 2007) to check population structure and ensure that individuals were not clustered by sex, which could bias the analysis. Additionally, we estimated relatedness between the individuals using the option “relatedness2” in vcftools (Manichaikul *et al.*, 2010): values close to 0.5 indicate clones, around 0.25 full siblings, and around 0.125 2nd-order relatives. Paralogous sequences can lead to relatedness overestimation as they harbor heterozygous sites across individuals. As SDpop detects potentially paralogous sequences (see below), if a dataset for a species had high paralogy rate we removed genes with paralogous posterior probabilities above 0.8 and re-estimated the relatedness.

Sex-linked genes

We used SDpop (Käfer *et al.*, 2021) to infer the presence and type (XY or ZW) of sex chromosomes, as well as to identify the sex-linked genes. The tool formalizes the population genetic concepts behind commonly used methods for sex-linkage detection such as male vs female F_{ST} or GWAS, and puts them in a probabilistic framework that accounts for some frequently encountered sources of error

(genotyping errors, paralogy and haploidy). It allows to detect sex linkage (i.e. gametology, XY or ZW, or hemizygosity, when Y or W copies are absent), by inferring the allele frequencies on the putative X and Y copies of the gene from the observed genotype frequencies among females and males. Each gene is assigned a posterior score for each of the segregation types (autosomal, paralog, haploid, XY and X-hemizygous). Genes with a posterior score for XY higher than 0.8 were considered putatively sex-linked. The estimated allele frequencies on the X and Y chromosomes are used by SDpop to reconstruct the X and Y consensus haplotypes of the gametologous genes. For this, we used the SDpop default parameters: if the estimated allele frequency was above 0.95, the allele was considered fixed; if it ranged between 0.6 and 0.95, the major allele was output; and sites with no allele at a frequency above 0.6 were considered missing ("N").

As SDpop's posterior scores for a gene are only based on the average allele-genotype frequency equilibria and not on SNP density, we used the latter to refine and confirm SDpop's results. First, we calculated the average per-gene heterozygosity of the individuals of each sex. As a statistic, we used the proportion of average male heterozygosity per gene, i.e. the average male heterozygosity divided by the sum of average female and average male heterozygosity. This proportion was plotted per gene, except for genes with no heterozygous positions.

Second, codeML (PAML version 1.9; Yang, 2007) was used to infer pairwise synonymous divergence (dS) between the inferred X and Y haplotypes. Sex-specific deviations in genotype frequencies can arise by chance or through linkage disequilibrium with the non-recombining region, but such genes will not have accumulated substitutions independently. Thus, we compared the dS of the putative sex-linked genes to the genome-wide heterozygosity in each species (using the median value of per-gene heterozygosity, excluding genes with paralogous or XY posterior scores over 0.8).

For comparative purposes, we focused on all genes that were putatively sex-linked (i.e. SDpop posterior XY score > 0.8) in at least one dataset, and categorized them as follows. Among the genes with posterior XY scores over 0.8, those that had a dS higher than the species' median heterozygosity were considered sex-linked with "high confidence" (HCSL), others were considered "probably sex-linked" (PSL). Equally, genes that had posterior XY scores between 0.5 and 0.8 were considered "probably sex-linked". Genes with autosomal posterior scores above 0.8 were considered as "not sex-

linked". Finally, if genes had on average fewer than 10 individuals genotyped per site, we could not assert sex-linkage or its absence and considered them "inconclusive". All genes not fitting any of the previous criteria were classified in the inconclusive category as well. These criteria are summarised in Table **S1**. When a gene was present in multiple datasets of the same species, we based this classification either on the dataset with most polymorphisms or, if equal, with more individuals genotyped on average.

We plotted the HCSL genes on the genomes of *P. dactylifera* (PDMBC4) and *E. guineensis* (EGPMv6), which are the most contiguous genomes assembled to date. Our aim was to determine whether these genes are clustered in a single genomic region or dispersed and to identify their syntenic region(s), if any, in a monoecious species (*E. guineensis*). To achieve this, we extracted coding sequences (CDS) from the reference genomes using gffread v.0.12.7 (Pertea & Pertea, 2020). The genome annotation files were converted from GFF to BED format and processed using JCVI functions in Python v. 3.12.7. Pairwise synteny analysis and visualization were performed using MCScan (Python version) (https://github.com/tanghaibao/jcvi/wiki/MCScan-(Python-version)).

Gene divergence and phylogeny

We identified genes in the *E. guineensis* genome that are homologous to inferred sex-linked genes by selecting the best hit in a blast search against NCBI's core nucleotide database. Sequences were aligned using muscle (Edgar, 2004), or PRANK (Löytynoja A, 2014) for alignments containing indels shifting the reading frame. Despite the absence of homologous recombination during meiosis, ectopic gene conversion could prevent divergence of the two gametologous copies (Jeffreys & May, 2004; Rosser *et al.*, 2009; Niederstätter *et al.*, 2013). Geneconv (Sawyer, 1989) was therefore used to detect gene conversion in these alignments. Geneconv identifies stretches with reduced divergence in alignments, indicative of recombination through gene conversion. Geneconv then calculates two p-values, simulated p-values are considered more accurate yet less conservative than Karlin-Altschul (KA) p-values. In order to avoid underestimating the age of recombination arrest of genes, we considered pairwise or global inner-fragments (respectively from one-to-one or one-to-all comparison among the sequences in the alignments) to have undergone gene conversion when at least one of the two p-values was lower than 0.05 between X and Y sequences from the same dataset. For *P. dactylifera*, the same fragment (same start and end position) of the gene was required to fit these criteria for both the Whole-

Genome Sequencing (WGS) and targeted-capture datasets.

The phylogeny was then inferred using BEAST2 v2.7.5 (Bouckaert *et al.*, 2019) with a GTR + Γ model with 4 gamma categories (Lanave *et al.*, 1984; Yang, 1993, 1994a, 1994b). The length of the chain was 250,000,000 steps and a sample was taken every 100 steps after a pre burn-in of 250 samples. A relaxed clock model was chosen (Drummond *et al.*, 2006). The prior for the most recent common ancestor (MRCA) age for the root was set to normal distribution with a mean of 87.025 and a standard deviation of 0.625 fitting the 95% confidence interval of this node age in previous dated phylogenies (Baker & Couvreur, 2013). Other parameters and priors were not modified. If convergence of the model was not reached, the length of the chain was increased and the program stopped after all parameters converged and reached an effective sample size (ESS) of 400 on Tracer v1.7.2 (Rambaut *et al.*, 2018). A maximum clade credibility tree was then generated with 10% burn in with node heights corresponding to MRCA age (Bouckaert *et al.*, 2019). The figures of the inferred trees were generated using ggtree v3.11.1 (Yu, 2020). We additionally used Yao *et al.* (2023) 'complete-105 regions matrix.300_105_result' plastid phylogenetic tree to recreate a genus-level phylogeny of palm sexual systems (Nadot *et al.*, 2016; Cássia-Silva *et al.*, 2021) for context.

Gene Ontology enrichment

We first updated the Gene Ontology (GO) annotation of the *P. dactylifera* genome (DPV01). Protein sequences were extracted from the genome using GffRead (Pertea & Pertea, 2020) and a functional annotation was elaborated using Fantasia with default parameters (Martínez-Redondo *et al.*, 2024). GO terms were filtered and manually curated based on scores calculated by Fantasia (filtration threshold of 0.3).

To investigate the enrichment of sex-related GO terms among genes identified in the suggested sex-linked region (see Results), we conducted a GO enrichment analysis using the topGO package in R version 2.58 (Alexa & Rahnenfuhrer, 2010). We considered the genes of interest, the set of 92 genes located in the proposed sex-linked region. Two distinct gene lists were used as reference universes: (i) all genes captured by the two sets of baits, which had at least one read coverage after mapping sequencing data to the targets, and (ii) genes with a minimum of seven reads coverage on the targets. The GO enrichment was elaborated for the go-category, biological process, using the topGO weight01 algorithm and the Fisher statistical test. The P-value < 0.05 was set as the cutoff for the significance of the gene enrichment. We note that the weight01 algorithm is an improved method that combines the

elim and weight algorithms (Alexa *et al.*, 2006; Grossmann *et al.*, 2007).

Results

Characterizing sex-linked genes in *P. dactylifera*

In *P. dactylifera*, the average mapping rates for the whole-genome sequencing data (WGS, Table **S2**), and SexPhoenix (SP) and PalmExons (PE) capture kits (Table **S3**), were 94.28%, 99.46% and 99.51%, respectively. Target capture covered 779 of the 832 targeted regions at a depth of over 1X with a median depth of 38.84 reads per base and a median coverage of 38.57% of the targets for SP. The PE kit captured 25,579 of the 29,983 targeted regions at a depth of over 1X with a median depth of 6.49 reads per base and a median coverage of 11.35% of the targets. Due to high relatedness between samples, we discarded three female and three male samples from the WGS data (Figure **S2a**,**S3a**, Table **S2**), and one male sample for the sequence capture data (Fig **S2b**,**S3b**, Table **S3**). Therefore, for the WGS data, the datasets consisted of 17 females and 9 males, while for both capture data (SP and PE), 9 individuals of each sex were included in the datasets analyses. After filtering by read depth (over 10 reads per site per individual for WGS data, over 7 for the capture kits), we analyzed over 450,000 SNPs and indels for the sex-linkage analysis in 25,100 genes (98% of the annotated protein-coding genes in the female date palm genome, DPV01, median gene length coverage over 99%) using the WGS data (Table **S4**). For the capture data, a total of 4,693 variant positions in the SP data covering 412 genes (1.6% of the annotated genes, median gene length coverage 75%) and 180,035 SNPs in the PE data covering 19,889 genes (77%, median gene length coverage 48%) were analyzed (Table **S4**).

Upon analysis of the WGS data with SDpop, 90% of the polymorphic sites were inferred to be autosomal (Table **S5**) while the proportions of haploid and sex-linked (XY gametologous and X-hemizygote) sites were inferred to be fewer than 1%. In the sequence capture datasets, fewer than 1% of sites were found sex-linked in PalmExons (Table **S5**), consistent with the WGS data proportions. As expected by design of the capture kits, the proportion of sex-linked sites within SexPhoenix baits was much higher, 12% (Table **S5**). Excluding genes with paralogous or XY posterior scores above 0.8 in SDpop, median per gene heterozygosity was 0.0021 for both WGS data (24,472 genes) and PE data (19,703 genes). We hence used 0.0021 as the synonymous divergence (dS) threshold value for high-confidence sex-linked genes (HCSL) in *P. dactylifera* (Table **S1**).

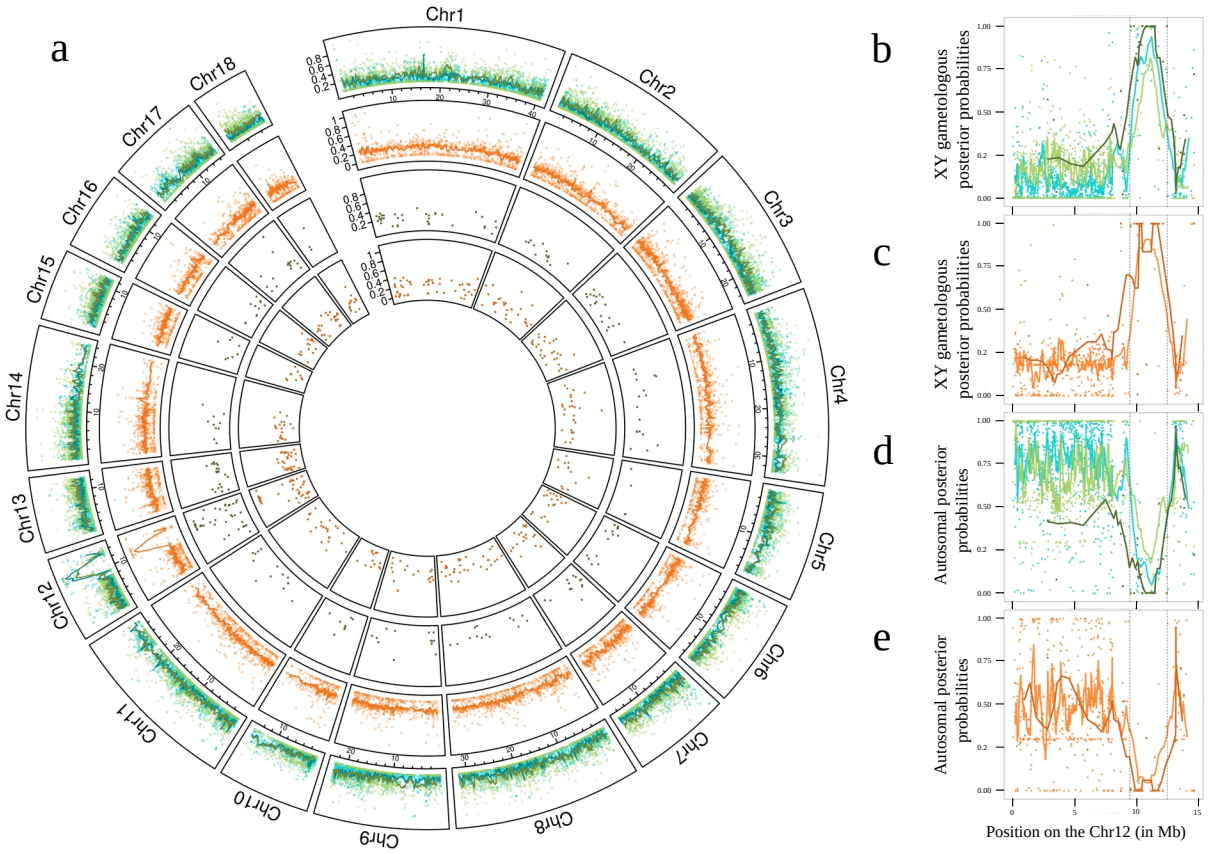

Figure 2. Probability of sex linkage (XY) of each gene for *Phoenix dactylifera* and *Kerriodoxa elegans*. The position of the genes is taken from the PDMBC4 assembly of *P. dactylifera* (Hazzouri *et al.*, 2019). *P. dactylifera* is indicated in blue (whole genome resequencing data) and green (capture kit data), *K. elegans* in orange. (**a**) Genome-wide distribution of XY posterior probabilities obtained with SDpop. Outer two rings show whole-genome resequencing and capture (PalmExons) data, the inner two the SexPhoenix capture kit. **(b,c)** XY posterior probabilities per gene on chromosome 12. **(d,e)** Autosomal posterior probabilities per gene on chromosome 12. Lines show the rolling mean with a window size of fifteen genes for the PalmExons kit (light green or orange) and whole genome resequencing data (blue) and five genes for the SexPhoenix kit (dark green or orange).

The highest XY scores inferred by SDpop for the *P. dactylifera* genes on the PDMBC4 genome (Fig. **2a**, outer ring) are on chromosome 12, the previously identified sex chromosome (Mathew *et al.*, 2014) (Fig. **2b**). A 3 Mb region between 9.4 Mb and 12.4 Mb on this chromosome mostly contains genes with high XY scores, while containing no genes for which autosomal segregation was inferred (Fig. **2d**). The location of the non-recombining region is also visible in a comparison of average female and male heterozygosity, with a strong increase in male heterozygosity as expected in an XY system (Fig. **S4**). We combined the results of WGS, PE and SP datasets by using the one with the most polymorphisms when a gene was present in multiple datasets (see Material and Methods). We thus classified 45 genes

as high-confidence sex-linked (HCSL), because they had SDpop XY posterior scores over 0.8 and X-Y dS higher than the average nucleotide diversity (0.0021, Table **S1**), both criteria being strong indicators of recombination suppression. We additionally classified 42 genes as probably sex-linked (PSL) when their dS was lower or when their probability to be XY was between 0.5 and 0.8. Among HCSL genes, 13 are on chromosome 12 and 26 on PDMBC4 unassigned scaffolds (File **S3**). Similarly, 15 PSL genes are on chromosome 12 and 18 on unplaced scaffolds (File **S3**). Few genes had posterior scores higher than 0.8 for X-hemizygosity (WGS, PE and SP), but upon verification, none of these genes had significant differences in female and male read coverage (File **S4**), so we conclude no X-hemizygous genes were detected.

Among the genes previously described as Y-specific in *P. dactylifera* (Torres *et al.*, 2018), only LOG3like (LOC103701078) was inferred as XY in our analysis (File **S3**). Further investigation confirmed this was due to paralogy of the Y-specific gene and an autosomal gene, as previously found (Torres *et al.*, 2018): males had more reads than females and reconstructed X and Y haplotypes aligned to two different loci in the date palm genome (LOC120104231 on chromosome 17 in the PDMBC4 assembly for the X sequence, and mRNA from the Y chromosome (MH685630) for the Y sequence). The duplication between the LOG autosomal and Y-linked copies is estimated at 53.76 My (Figure **S5**), likely predating sex-linkage. Concerning the other two Y-specific genes identified previously, we confirmed by remapping previously unmapped reads (i.e. those that did not align to the female DPV01 genome) to the PDMBC4 genome that both GPAT3 (LOC120108105) and CYP703 (LOC120107104) had no female reads for *P. dactylifera* (File **S3**). Thus, our approach based on target capture sequencing and sex-linkage identification in *P. dactylifera* using SDpop leads to similar results as previous studies.

K. elegans **and** ***P. dactylifera*** **sex chromosomes share sex-linked genes and a common genomic region**

The capture sequences of *K. elegans* had 83.95% of properly-paired reads for SP and 99.20% for PE when mapped on the DPV01 female *P. dactylifera* genome. Most *K. elegans* samples were related, with initial analyses suggesting they are full siblings (Figure **S2b,S3b**), but after removing possibly paralogous genes from the data (genes with SDpop's paralogous posterior scores over 0.8), most individuals were inferred to be first-degree cousins (Figure **S6**). Some inbreeding is expected as *K.*

elegans has small populations and many samples come from botanical gardens. This will have a negligible effect on the inference of sex-linkage as relatedness was found between female and male individuals alike, and our inferences were based on population genetic equilibria as well as dS between X- and Y-copies, and the latter is not affected by relatedness. SDpop was run on 14 females and 11 males of *K. elegans* with 161,384 variant positions for PE covering 15,051 genes (58% of the DPV01 annotated genes, median gene length coverage 43%) and 8,395 variant positions covering 655 genes (2.5%, median gene length coverage 54%) for SP (Tables **S3,S4**).
As sex chromosomes were not previously known in *K. elegans*, we ran SDpop's models for XY sex chromosomes, ZW chromosomes and without sex-linkage. The model that most accurately fitted both datasets of *K. elegans* according to the Bayesian Information Criterion (BIC) is XY (Table **S5**), i.e. the same as *P. dactylifera*. Median heterozygosity per gene was 0.0011 in PE data excluding genes with XY or paralogous scores above 0.8 (13,442 genes). Thus, 0.0011 was used as the dS threshold value for *K. elegans* HCSL genes (Table **S1**).

When a gene was present in both datasets, we used the data from the dataset in which it had the most polymorphisms for subsequent analysis. We identified 59 HCSL genes in *K. elegans*, 25 on chromosome 12, 4 on other linkage groups, 29 on unplaced scaffolds and 1 not positioned on the PDMBC4 assembly (Figure **2**, File **S3**). SD-pop analysis suggested that some genes could be X-hemizygous but after analysis of the female and male coverage, this could not be confirmed (File **S4**). Most genes found to be sex-linked in *P. dactylifera* and *K. elegans* were common between the two species, even those on unplaced scaffolds (Figure **2**, Figure **S4**, File **S3**). More precisely, of the 45 genes inferred as HCSL in *P. dactylifera* and the 59 in *K. elegans*, 21 were so in both species, whereas only 2 HCSL genes in *P. dactylifera* and 10 in *K. elegans* were found to be autosomal in the other species (File **S3**). Furthermore, 15 HCSL genes in *K. elegans* were probably sex-linked (PSL) in *P. dactylifera*, and three HCSL genes in *P. dactylifera* were PSL in *K. elegans* (Fig. **3**, File **S3**). Mapping previously unmapped reads to the PDMBC4 male genome revealed that two Y-specific genes of *P. dactylifera*, GPAT3 (LOC120108105) and CYP703 (LOC120107104), were XY in *K. elegans*. The third Y-specific gene of *P. dactylifera*, LOG3like (LOC103701078), was inferred as autosomal in *K. elegans* (File **S3**).

As the PDMBC4 assembly was generated using a male individual, a considerable fraction of the non-

recombining region might have been difficult to assemble. However, the sex-linked region in *P. dactylifera* shares synteny with a genomic region on the monoecious oil palm (*Elaeis guineensis*) chromosome 10 (Fig. 3a), so we positioned the sex-linked genes of *P. dactylifera* and *K. elegans* on the *E. guineensis* EGPMv6 genome. They indeed fall in a single region between 43 and 46.1 Mb of the *E. guineensis* chromosome 10, in a more contiguous pattern than in PDMBC4 genome (Fig. **3**, table **S6**). In total, this region contains 108 protein-coding genes according to the EG5 annotation for *E. guineensis* and 95 according to the DPV01 annotation for *P. dactylifera,* with the addition of two Y-specific genes from the PDMBC4 annotation (Figure **S7**). It contains 78% of genes inferred as HCSL in either *P. dactylifera* or *K. elegans*, including 90% of common HCSL genes. None of the genes in this region were inferred to be autosomal in *K. elegans*, while 17 were in *P. dactylifera* (Fig. **3**, Table **S7**, File **S3**), indicating that the sex-linked region in *K. elegans* might be slightly larger.

To determine if the sex-linked region was enriched in genes related to sex determination, we first improved the functional annotation of the DPV01 genome assembly. The updated annotation resulted in the annotation of 24,625 genes (ca. 80% of the genome). The *de-novo* functional annotation was compared and merged with the annotation of *P. dactylifera* PDMBC4 genome. The final annotation encompasses GO IDs for 29,167 genes, covering approximately 95% of the DPV01 genome (File **S5**). We then performed GO enrichment analysis on all 92 protein-coding genes between 43.3Mb and 46.1Mb on chromosome 10 of *E. guineensis* (excluding the 43Mb to 43.3Mb region as it contains genes that are only sex-linked in *K. elegans*; Fig. **3b**, File **S3**). The analysis showed highly similar results when taking into consideration the genome-wide captured genes (universe genes) with 1X and 7X read coverage (File **S6**). We identified a significant enrichment of GO terms ($p < 0.05$) covering various biological processes, including DNA repair, stress responses, and protein translation (File **S6**). While a few GO terms related to plant reproductive mechanisms, such as pollen tube adhesion, plant ovule development, specification of floral organ identity, and auxin-activated signaling pathway, showed significant enrichment ($p < 0.05$), the copy number of genes associated with these terms was not overrepresented which reduces the statistical significance of enrichment for these genes (File **S6**). Therefore, our analysis did not reveal convincing sign of the over-representation of GO terms for genes with floral development or sex-linked functions.

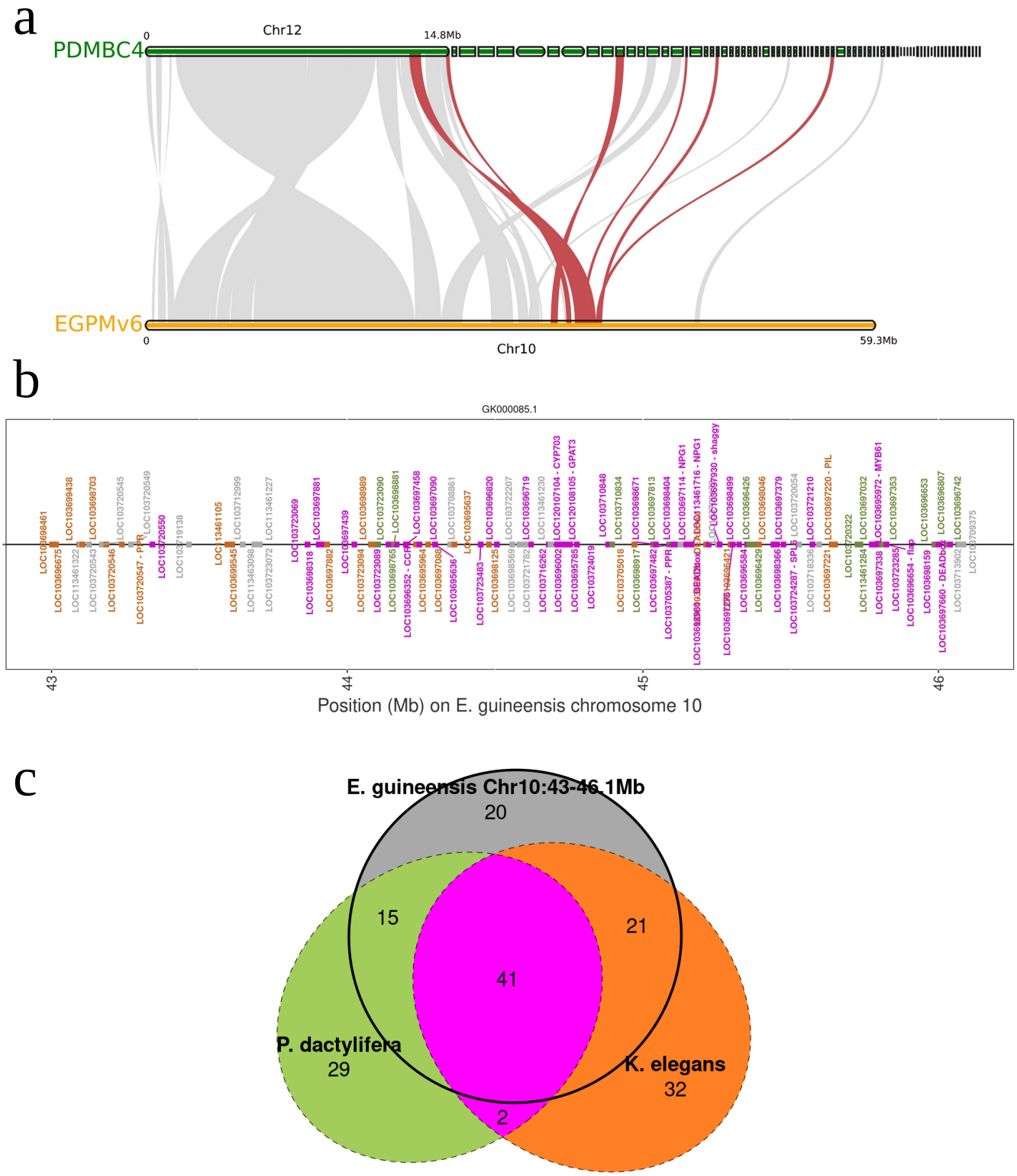

Figure 3. Position of *Kerriodoxa elegans* and *Phoenix dactylifera* sex-linked genes on *Elaeis guineensis* chromosome 10. Genes with posterior probability to be XY above 0.8 in at least one dataset or present between 43 and 46.1Mb on chromosome 10 of the *E. guineensis* EGPMv6 genome

were categorized as follows: high-confidence sex-linked, probably sex-linked, inconclusive, not sex-linked or missing data. **(a)** Synteny between *E. guineensis* EGPMv6 chromosome 10 (orange) and *P. dactylifera* PDMBC4 chromosome 12 and several unplaced scaffolds (green). Synteny of sex-linked genes is colored in red. **(b)** Positions of genes between 43 and 46.1Mb on chromosome 10 of *E. guineensis*. Sex-linked genes are colored in green for *P. dactylifera*, orange for *K. elegans*, and magenta for both. Genes from other categories (i.e. either inconclusive, or absent in at least one species, or autosomal in at most one) are colored in grey. **(c)** Euler diagram of the number of sex-linked genes (HCSL and PSL) in *P. dactylifera* (green) or *K. elegans* (orange) or positioned between 43 and 46.1Mb on the chromosome 10 of *E. guineensis* (grey).

Independent recombination arrest for *P. dactylifera* and *K. elegans*

To investigate whether recombination suppression took place in a common ancestor of *Kerriodoxa* and *Phoenix*, we inferred the gene trees and divergence times for the 42 genes that were found to be sex-linked in both species (either HCSL in both species or HCSL in one and PSL in the other, see Figure **3b**, File **S4**), using the X and Y consensus haplotypes inferred using SDpop, and *E. guineensis* as an outgroup. Prior to the analysis, we found possible gene conversion in 3 genes in *K. elegans* and 3 different ones in *P. dactylifera* (Table **S8**). The effect of either retaining or removing these stretches on the inferred divergence times is negligible (Figure **S8**); for further analyses, we nevertheless chose to discard these stretches.

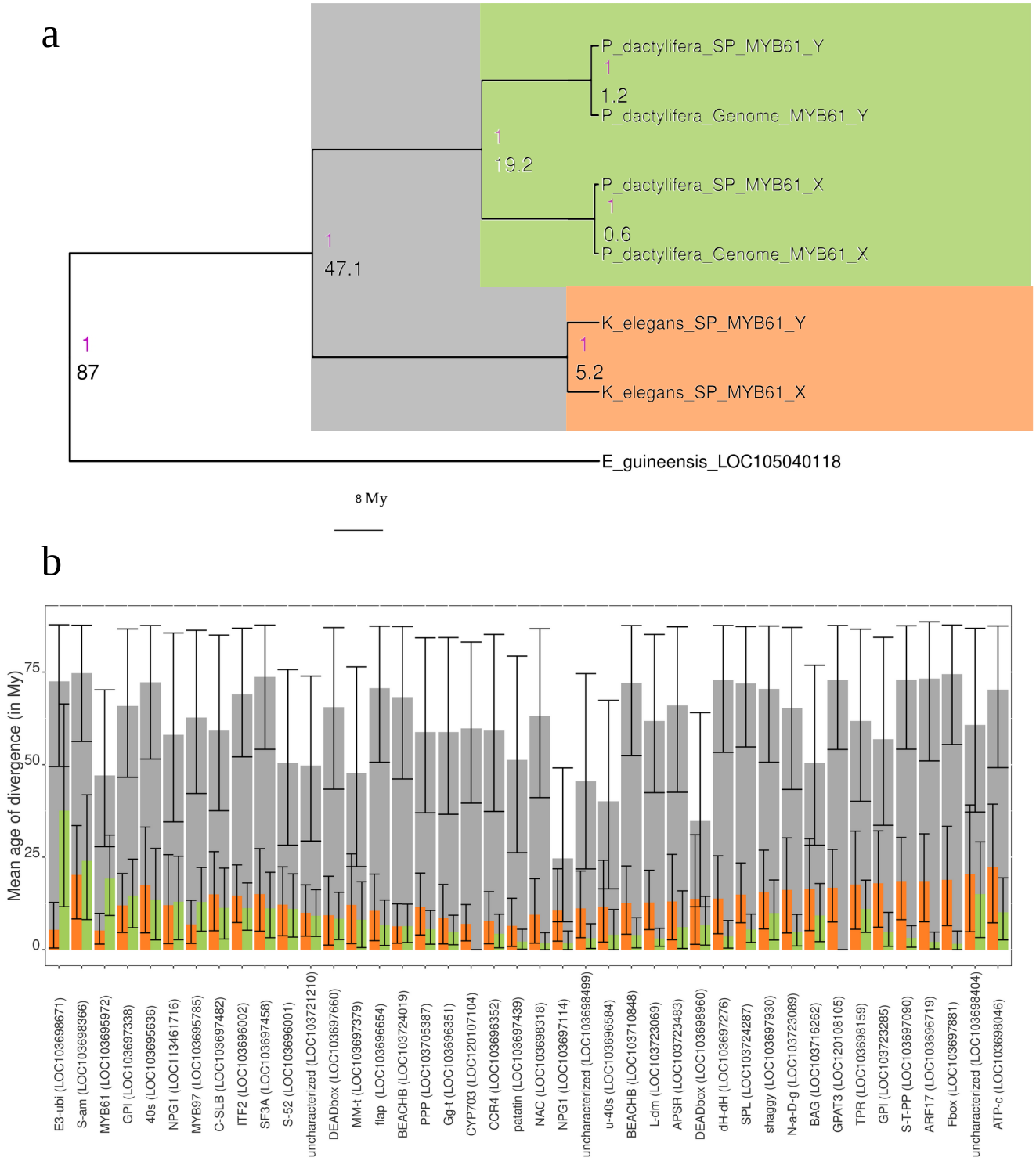

Figure 4. Ages of species and gametolog divergence for common sex-linked genes in *Phoenix dactylifera* and *Kerriodoxa elegans*. Age estimates are colored in grey for the divergence of the *Phoenix* and *Kerriodoxa* lineages, in green for *P. dactylifera* X-Y divergence and in orange for *K. elegans* X-Y divergence. **(a)** Phylogenetic tree for the MYB61 (LOC103695972). Node values correspond to the mean age for the node's most recent common ancestor (MRCA; black) and the support of the node (magenta). **(b)** Mean age of divergence of X and Y sequences for common sex-

linked genes compared to the age of divergence between the MRCA of *P. dactylifera* and *K. elegans*. Error bars correspond to the 95% probability density of the node age.

In all phylogenetic trees, the X and Y sequences from each dioecious species formed a strongly supported clade (Fig. **4a**, **S5**), indicating that recombination suppression evolved after the divergence of the *Phoenix* and *Kerriodoxa* lineages. The node ages in these 42 sex-linked gene trees, that were calibrated using previously estimated divergence times at the level of the palms family, confirmed that recombination suppression occurred much later than the split between the *Phoenix* and *Kerriodoxa* lineages (Fig. **4b**). The mean age of divergence between *P. dactylifera* and *K. elegans* is 61.86 My, whereas mean ages of X-Y haplotypes splitting for the five most divergent genes of each species were estimated to be 22.07 My for *P. dactylifera* and 19.32 My for *K. elegans* (Fig. **4b**). Thus, despite the similarity in gene content and age of these regions, none of the common genes in the sex-linked region showed any evidence of recombination suppression in the last common ancestor of *P. dactylifera* and *K. elegans*. Among the genes that were sex-linked in only one species, we did not observe substantially higher X-Y dS values than for common sex-linked genes (File **S4**), indicating that none of the species-specific sex-linked genes stopped recombining earlier. We conclude that the sex chromosomes of *P. dactylifera* and *K. elegans* evolved independently, which is congruent with the ancestral state reconstructions of sexual systems (Fig. **1**).

Synonymous divergence between the X and Y copies of sex-linked genes is rather low, typically lower than 3%, which is strikingly different from a species like *Silene latifolia* which has about 10% synonymous divergence for 11 My of divergence (Krasovec *et al.*, 2018). We investigated whether divergence of sex-linked genes with their *E. guineensis* homologs was different than for autosomal genes, using 18 genes that were sex-linked in both species (using SP data which covers a larger part of the genes in this region, Figure **S9**, Table **S4**) as well as ten random autosomal genes from the BUSCO *Liliopsida* database (Table **S9**). Cumulated synonymous divergence (dS) with *E. guineensis* was similar for autosomal and sex-linked genes (Figure **S9**), indicating that the sex-linked genes experienced substitutions at similar rates as autosomal genes. This was expected based on the relatively short time for which these genes have stopped recombining.

Discussion

A sex-linked region recruited independently in two distantly related palm species

Based on exon target-capture sequencing and subsequent analyses, we show that *Kerriodoxa elegans* and *Phoenix dactylifera*, two palm species that diverged approximately 66 My ago, have similar XY sex-linked regions. The estimated ages of recombination suppression in both species show that these sex-linked regions evolved independently between 10 and 40 My ago, in line with ancestral state reconstructions of the sexual systems that suggest that both species most likely evolved dioecy independently from hermaphroditism (Figure **1**; Nadot *et al.*, 2016; Cássia-Silva *et al.*, 2021). Despite their independent origins, *P. dactylifera* and *K. elegans* sex-linked regions exhibit striking similarities, including their size, relatively low divergence considering the age of recombination suppression, and minimal degeneration (no loss of Y genes), although the region might be slightly larger in *K. elegans*. Such convergent evolution seems unique among known plant sex chromosomes.

In animals, gonochorism (sex separation) is ancestral in many taxa, but how sex is determined varies widely, and sex chromosomes have evolved many times independently (Bachtrog *et al.*, 2014). Convergent evolution of sex chromosomes has been reported in a few animal clades. For example, in *Xenopus*, it has been suggested that sex chromosome convergence arises due to frequent turnovers, with homologous regions containing key sex-linked genes shared among distant species (Furman & Evans, 2016). Indeed, in animals, gonadal developmental pathways are highly conserved, with similar precursors found in both invertebrates and vertebrates (Kopp, 2012), probably due to the fact that gonochorism is their ancestral state. Consequently, Dmrt and SOX genes have independently evolved multiple times to serve as sex determinants (Kopp, 2012). The mere presence of Dmrt1, or copies of it, on a chromosome makes it likely to evolve into a sex-determining gene, as seen repeatedly in amniotes (O'Meally *et al.*, 2012; Ezaz *et al.*, 2017).

In plants, dioecy evolved many times independently, and sex determination mechanisms have long been thought to be very diverse (Mitchell & Diggle, 2005; Henry *et al.*, 2018). However, as for animals, it is widely accepted that plant sex-determining regions (SDRs) or sex chromosomes contain critical genes involved in sexual differentiation and the development of sex-specific traits. These genes often serve as key regulators in pathways that establish and maintain dioecy, underpinning the evolutionary significance of SDRs in controlling sex-specific phenotypes, and recent progress suggests that several pathways could be common among distantly related plant species (cf Leite Montalvao *et*

al., 2021).

The shared sex-linked region contains genes related to flower sexual development

It seems highly unlikely that a single, 3 Mb region evolved recombination suppression twice just by chance. Recombination suppression is believed to originate with at least one sex-determining gene, implying that the sex-determining genes in both species are located within this region. Which genes, then, are present in this region and could account for its independent recruitment in the two species?

While a GO term analysis of the sex-linked region did not convincingly demonstrate an over-representation of genes involved in plant reproductive development, we identified several potentially interesting genes with functions in flower and sexual organ development based on gene annotations. A substantial number of genes has been found to be involved in pollen and anther development and male sterility in a range of other plants, and a few other genes are involved in ovule development, hormone signaling and inflorescence branching (Table **1**). In *P. dactylifera*, Torres *et al.* (2018) proposed a hypothesis for the evolution of dioecy and sex chromosomes, identifying three Y-specific genes. Among these, *GPAT3*, a glycerol-3-phosphate acyltransferase, and *CYP703*, a member of the cytochrome P450 subfamily, are crucial for anther and pollen development and male fertility in monocot species (Yang X *et al.*, 2014; Li & Liu, 2017; Somaratne *et al.*, 2017; Xie *et al.*, 2018). Another gene, *LOG3*, belongs to the LONELY GUY (LOG) gene family, which is involved in cytokinin activation and ovule development in female flowers (Kurakawa *et al.*, 2007; Yamaki *et al.*, 2011). Loss of male function in some individuals could have led to gynodioecy (involving recessive loss-of-function of *GPAT3* and/or *CYP703*), followed by the loss of female function (dominant suppression by LOG3) leading to dioecy in date palm (Torres *et al.*, 2018). Although our methods were not primarily designed to detect Y-specific genes, additional analyses confirmed these genes are Y-specific in *P. dactylifera*. In *K. elegans*, however, *GPAT3* and *CYP703* were inferred as XY gametologs, and *LOG3* as autosomal. Furthermore, the X-Y copy divergence of these genes in *K. elegans* was not among the highest values found for this species, suggesting that they have been recruited after initial recombination suppression involving the sex-determining gene(s) in this species. While functional analyses of sex-linked genes have yet to be conducted in both species, these findings suggest that the master sex-determining genes in *K. elegans* are different from those in *P. dactylifera*.

The role of hormones (cytokinins, auxins and jasmonate) in palm sex differentiation has been

demonstrated in the monoecious species *Elaeis guineensis* and *Areca catechu* through content variations between female and male inflorescences (Tregear *et al.*, 2022; Zhou *et al.*, 2022). In *E. guineensis*, an antagonistic regulatory model has been proposed for both sexual differentiation and branching activity in inflorescences, as male inflorescences have more primary branches than female ones (Tregear *et al.*, 2022). This model involves the *LOG* gene, the *SQUAMOSA PROMOTER-BINDING PROTEIN-LIKE* (*SPL*) gene, which plays a role in inflorescence development and branching (Kellogg, 2022), and the *PHYTOCHROME-INTERACTING FACTOR-LIKE* (*PIL*) family of transcription factors, which directly interact with SPLs to repress branching and tillering (Zhang *et al.*, 2022). *E. guineensis* female inflorescence development is characterized by cytokinin accumulation, increased expression of *LOG* and *SPL* genes, and reduced levels of miRNA regulators, while male inflorescences exhibit higher auxin levels and increased expression of *PIL* genes (Tregear *et al.*, 2022). As genes similar to *SPL*, *PIL* and *LOG3* are sex-linked in *P. dactylifera* and/or *K. elegans* (Table **1**), the same genes could be involved in flower sex determination in monoecious palm species and sex determination at the whole-plant level in dioecious species. Not all these genes need to be present in the sex-determining region, as one of them could act as a master-switch gene and also control expression of autosomal genes that are involved in the pathway. The fact that the same genomic region has been recruited twice indicates that it is rich in such potential master-switch genes.

The sex-linked region in *P. dactylifera* and *K. elegans* has conserved synteny since its split with *E. guineensis*. This region has furthermore been shown to be syntenic in two other monoecious species, *Cocos nucifera* and *Areca catechu* (Zhou *et al.*, 2022). It was therefore probably present in the common ancestor of the Arecoideae (to which *E. guineensis*, *C. nucifera* and *A. catechu* belong) and the Coryphoideae (with *P. dactylifera* and *K. elegans*) subfamilies, estimated to be 87 My old (Baker & Couvreur, 2013). Considering its composition in sex-related genes, we hypothesize that this region could act as a "genetic toolbox" for the development of unisexual flowers in palms. It could play a key role in facilitating transitions between monoecy, dioecy, and hermaphroditism, even if the master sex-determining genes might be different. It is noteworthy that palms represent one of the plant families with the highest proportion of unisexual flowers, with around 80% of species, compared to only about 10% across angiosperms, and have undergone many transitions between sexual systems (Nadot *et al.*, 2016). Genomic colocalization of genes involved in the same pathway could facilitate concerted regulation (Hurst *et al.*, 2004) and thus evolutionary transitions involving the pathway. Interestingly, a region responsible for sex determination in *Vitis* was recently shown to constitute a conserved collinear

region specific to flowering plants, containing many genes related to flower development (Massonnet *et al.*, 2024). Currently, however, and by contrast to the "toolbox" region in palms, it is not known to have given rise to sex chromosomes following other transitions to dioecy.

Palms as a model system for sex chromosome evolution

Our findings raise the question whether the region we identified in *P. dactylifera* and *K. elegans* might have given rise to sex chromosomes in other palm species. We here also presented the approach that could be used to answer this question. Palms are a large, mostly tropical family for which only a few, economically important species have been studied. They often exhibit large genome sizes: the ancestral genome size was approximately 3.6 Gb, with some species reaching genome sizes as large as 29 Gb (Barrett *et al.*, 2019). Despite the increasing accessibility of long-read genome sequencing and assembly, studying many species that cannot be easily bred in the lab remains challenging, especially when genome sizes are large. Sex chromosomes raise particular difficulties associated with divergence, transposable elements, and inversions (Carey *et al.*, 2022; Hobza *et al.*, 2024). Indeed, we have shown that more than half the genes that are probably part of *P. dactylifera* sex-linked region were not placed on the latest genome pseudomolecules (Hazzouri *et al.*, 2019). To investigate sex linkage in multiple dioecious palm species with limited genomic resources, we developed a method based on the reduction of genome complexity (Fig. **S1**). This approach uses sequence capture datasets designed mainly from the female date palm genome (DPV01) and targets either previously identified sex-linked regions (SexPhoenix, SP) or exonic sequences (PalmExon, PE). This latest target capture set provides genomic information on 20,000 genes in *P. dactylifera*, as well as 15,000 genes in *K. elegans*, despite their 66 million years divergence. As coding sequences are generally relatively well conserved at the level of a plant family, this approach allows investigating palm species in a cost-effective manner.

Our approach also incorporates the recently developed tool SDpop, specifically designed to identify and study sex-linkage in non-model species, requiring only a small number of individuals from which material can be collected in the wild, as long as sex can be phenotypically determined (Käfer *et al.*, 2021). SDpop assigns a probability to be sex-linked to genes and allows further investigation, by reconstructing their X and Y sequences from which divergence can be inferred. The use of both the posterior scores and X-Y divergence increases the robustness of the method. The genes found to be sex-linked are then positioned onto the date palm genome and genetic map to identify the sex-linked regions and sex chromosomes. The localization of the majority of sex-linked genes within a single

genomic region reinforces the confidence in the results. We showed this strategy is effective, successfully reproducing previous findings on *Phoenix dactylifera* sex chromosomes (Mathew *et al.*, 2014; Torres *et al.*, 2018; Hazzouri *et al.*, 2019), and identifying the sex chromosomes in a distantly related species, *Kerriodoxa elegans*, without prior knowledge. This approach does not provide a full picture of the sex chromosomes, as haplotype-aware genome sequencing and assembly would be able to provide, but can be used as a first comparative analysis of dioecious species, giving insights in the number and identity of sex-linked genes and sequence divergence.

Given the importance of several palm species as vital crops, where only females produce fruits and seeds, these genes could be used to develop genetic sex markers that allow early selection of female plants with high added value, thereby avoiding to wait before the sexual phenotype becomes apparent, which can take up to 15 years (Cherif *et al.*, 2013). More broadly, the existence of a region determining the unisexuality of inflorescences and the knowledge of the genes it contains offer perspectives for controlling the sex ratio of cultivated palm species, whether they are dioecious or monoecious (Ong *et al.*, 2020).

Table 1. Sex-linked genes with functions related to flower development.

P. dactylifera gene	Putative gene function in sex	Function group	*P. dactylifera* category	*K. elegans* category
CCR4-not (LOC103696352) transcription complex subunit 9-like	Anther development (Sun *et al.*, 2018)	Male sterility	Probably XY	XY
CYP703 (LOC120107104) cytochrome P450 703A2	Pollen and anther development (Yang X *et al.*, 2014; Somaratne *et al.*, 2017)	Male sterility	Y specific	XY
DEAD-box ATP-dependent RNA helicase 40 (LOC103699024)	Male sterility linked to tapetum degeneration (Li X *et al.*, 2011)	Male sterility	inconclusive	XY
DEAD-box ATP-dependent RNA helicase 3B (LOC103697660)	Male sterility linked to tapetum degeneration (Li X et al., 2011)	Male sterility	XY	XY
DEAD-box ATP-dependent RNA helicase protein DB10 (LOC103698960)	Male sterility linked to tapetum degeneration (Li X et al., 2011)	Male sterility	Probably XY	XY
flap endonuclease 1A (LOC103696654)	Early microspore development (Moritoh *et al.*, 2005)	Male sterility	XY	XY
GPAT3 (LOC120108105) glycerol-3-phosphate acyltransferase RAM2-like	Pollen and anther development (Li & Liu, 2017)	Male sterility	Y specific	XY
MYB101 (LOC103695785) transcription factor MYB101	Male reproductive development (Wang Y *et al.*, 2023)	Male sterility	XY	Probably XY
MYB61 (LOC103695972) transcription factor MYB61	Male reproductive development (Wang Y et al., 2023)	Male sterility	XY	XY
NPG1-like protein (LOC103697114)	Pollen germination (Shin *et al.*, 2014)	Male sterility	Probably XY	XY
NPG1-like protein (LOC113461716)	Pollen germination (Shin et al., 2014)	Male sterility	XY	Probably XY
PPR At1g02420 (LOC103705387)	Cytoplasmic male sterility (Kitazaki *et al.*, 2023)	Male sterility	XY	XY
PPR At3g14580 (LOC103720547)	Cytoplasmic male sterility (Kitazaki et al., 2023)	Male sterility	Autosomal	XY
SPL6 (LOC103724287) squamosa promoter-binding-like protein 6	Anther development and male fertility (Xing S *et al.*, 2010)	Male sterility	Probably XY	XY
ARF17 (LOC103696719) auxin response factor 17-like	Anther development and male fertility (Yang J *et al.*, 2013)	Male sterility / Hormonal signaling	Probably XY	XY
ABC transporter C 1 (LOC103697353)	Gynoecious sex expression (Vinay *et al.*, 2023)	Female sterility	XY	inconclusive
LOG3 (LOC103701078) cytokinin riboside 5'-monophosphate phosphoribohydrolase	Female flower development (Kurakawa *et al.*, 2007; Yamaki *et al.*, 2011)	Female sterility / Hormonal signaling	Y specific	Autosomal
PIL (LOC103697220) transcription factor phytochrome interacting factor-like 15-like	Interacts with SPL and involved in rice panicle branching. (Zhang *et al.*, 2022)	Branching	Autosomal	XY
shaggy-related protein kinase alpha-like (LOC103697930)	rice panicle branching (Li & Liu, 2017; Zhang *et al.*, 2024)	Branching	XY	XY

Sex-linked genes in either *Phoenix dactylifera* or *Kerriodoxa elegans* with identified functions related to sexual development are listed, as well as their position on the *Elaeis guineensis* EGPMv6 genome. The level of confidence according to our analysis (Material and Methods) is indicated, as well as the reference for the function.

Acknowledgements

This project (ID 2101-014 and ID 2201-007) was funded through LabEx AGRO 2011-LABX-002 (under I-site Muse framework) coordinated by Agropolis Fondation. We thank Mike Dahme, Central Florida Palm and Cycad Society, USA for providing *Kerriodoxa elegans* material. We also thank the ISO 9001 certified IRD i-Trop HPC (South Green Platform) at IRD Montpellier for providing HPC resources that have contributed to the research results reported within this paper, as well as Audrey Weber from the Genotyping platform, INRAe Arcad AGAP, for sequencing.

Competing interests

The authors declare no conflict of interest

Author contributions

FA conceived the project. FA and JK supervised this study. ALe and ALi sampled the sequenced palms. SS performed the experiments. EC and FA designed the sequence capture. HT, JK, JO and PF performed the analyses of the genomic sequence. HT, JK, FA and PF wrote the manuscript. TB, JK and FA acquired funding. All authors read and approved the final manuscript. JK and FA contributed equally to this work.

Data and materials availability:

Raw reads data are available under the EBI Project PRJEB76653

Reference

Al-Dous EK, George B, Al-Mahmoud ME, Al-Jaber MY, Wang H, Salameh YM, Al-Azwani EK, Chaluvadi S, Pontaroli AC, DeBarry J, *et al.* 2011. De novo genome sequencing and comparative genomics of date palm (Phoenix dactylifera). *Nature Biotechnology* **29**: 521–527.

Alexa A, Rahnenfuhrer J. **2010**. topGO: enrichment analysis for gene ontology. *R package version* **2**: 2010.

Alexa A, Rahnenführer J, Lengauer T. **2006**. Improved scoring of functional groups from gene expression data by decorrelating GO graph structure. *Bioinformatics* **22**: 1600–1607.

Al-Mssallem IS, Hu S, Zhang X, Lin Q, Liu W, Tan J, Yu X, Liu J, Pan L, Zhang T, *et al.* 2013. Genome sequence of the date palm Phoenix dactylifera L. *Nature Communications* **4**: 2274.

Bachtrog D, Mank JE, Peichel CL, Kirkpatrick M, Otto SP, Ashman T-L, Hahn MW, Kitano J, Mayrose I, Ming R, *et al.* 2014. Sex Determination: Why So Many Ways of Doing It? *PLoS Biology* **12**: e1001899.

Baker WJ, Couvreur TLP. **2013**. Global biogeography and diversification of palms sheds light on the evolution of tropical lineages. I. Historical biogeography (WD Kissling, Ed.). *Journal of Biogeography* **40**: 274–285.

Balounova V, Gogela R, Cegan R, Cangren P, Zluvova J, Safar J, Kovacova V, Bergero R, Hobza R, Vyskot B, *et al.* 2019. Evolution of sex determination and heterogamety changes in section Otites of the genus Silene. *Scientific reports* **9**: 1045.

Barrett CF, McKain MR, Sinn BT, Ge X-J, Zhang Y, Antonelli A, Bacon CD. **2019**. Ancient Polyploidy and Genome Evolution in Palms. *Genome Biology and Evolution* **11**: 1501.

Bouckaert R, Vaughan TG, Barido-Sottani J, Duchêne S, Fourment M, Gavryushkina A, Heled J, Jones G, Kühnert D, Maio ND, *et al.* 2019. BEAST 2.5: An advanced software platform for Bayesian evolutionary analysis. *PLOS Computational Biology* **15**: e1006650.

Carey SB, Lovell JT, Jenkins J, Leebens-Mack J, Schmutz J, Wilson MA, Harkess A. **2022**. Representing sex chromosomes in genome assemblies. *Cell Genomics* **2**: 100132.

Cássia-Silva C, Freitas CG, Jardim L, Bacon CD, Collevatti RG. **2021**. In situ radiation explains the frequency of dioecious palms on islands. *Annals of Botany* **128**: 205–215.

Charlesworth B, Charlesworth D. **1978**. A Model for the Evolution of Dioecy and Gynodioecy. *The American Naturalist* **112**: 975–997.

Charlesworth D, Harkess A. **2024**. Why should we study plant sex chromosomes? *The Plant cell* **36**: 1242–1256.

Cherif E, Zehdi S, Castillo K, Chabrillange N, Abdoulkader S, Pintaud J, Santoni S, Salhi-Hannachi A, Glémin S, Aberlenc-Bertossi F. **2013**. Male-specific DNA markers provide genetic evidence of an XY chromosome system, a recombination arrest and allow the tracing of paternal lineages in date palm. *New Phytologist* **197**: 409–415.

Cherif E, Zehdi-Azouzi S, Crabos A, Castillo K, Chabrillange N, Pintaud J-C, Salhi-Hannachi A, Glémin S, Aberlenc-Bertossi F. **2016**. Evolution of sex chromosomes prior to speciation in the dioecious *Phoenix* species. *Journal of Evolutionary Biology* **29**: 1513–1522.

Comer J, Zomlefer W, Barrett C, Stevenson D, Heyduk K, Leebens-Mack J. **2016**. Nuclear phylogenomics of the palm subfamily Arecoideae (Arecaceae). *Molecular Phylogenetics and Evolution* **97**: 32–42.

Danecek P, Auton A, Abecasis G, Albers CA, Banks E, DePristo MA, Handsaker RE, Lunter G, Marth GT, Sherry ST, *et al.* 2011. The variant call format and VCFtools. *Bioinformatics* **27**: 2156–2158.

Dransfield J. **1983**. Kerriodoxa, a New Coryphoid Palm Genus from Thailand. *Principes* **27**: 3–11.

Drummond AJ, Ho SYW, Phillips MJ, Rambaut A. **2006**. Relaxed Phylogenetics and Dating with Confidence. *PLOS Biology* **4**: e88.

Edgar Rc. **2004**. MUSCLE: multiple sequence alignment with high accuracy and high throughput. *Nucleic acids research* **32**: 1792–1797.

Ezaz T, Srikulnath K, Graves JAM. **2017**. Origin of Amniote Sex Chromosomes: An Ancestral Super-Sex Chromosome, or Common Requirements? *Journal of Heredity* **108**: 94–105.

Furman Bls, Evans Bj. **2016**. Sequential Turnovers of Sex Chromosomes in African Clawed Frogs (Xenopus) Suggest Some Genomic Regions Are Good at Sex Determination. *G3 (Bethesda, Md.)* **6**: 3625–3633.

Grossmann S, Bauer S, Robinson Pn, Vingron M. **2007**. Improved detection of overrepresentation of Gene-Ontology annotations with parent child analysis. *Bioinformatics (Oxford, England)* **23**: 3024–3031.

Hazzouri KM, Gros-Balthazard M, Flowers JM, Copetti D, Lemansour A, Lebrun M, Masmoudi K, Ferrand S, Dhar MI, Fresquez ZA, *et al.* 2019. Genome-wide association mapping of date palm fruit traits. *Nature Communications* **10**: 4680.

Henry IM, Akagi T, Tao R, Comai L. **2018**. One Hundred Ways to Invent the Sexes: Theoretical and Observed Paths to Dioecy in Plants. *Annual Review of Plant Biology* **69**: 553–575.

Heyduk K, Trapnell DW, Barrett CF, Leebens-Mack J. **2016**. Phylogenomic analyses of species relationships in the genus *Sabal* (Arecaceae) using targeted sequence capture. *Biological Journal of the Linnean Society* **117**: 106–120.

Hobza R, Bačovský V, Čegan R, Horáková L, Hubinský M, Janíček T, Janoušek B, Jedlička P, Kružlicová J, Kubát Z, *et al.* 2024. Sexy ways: approaches to studying plant sex chromosomes. *Journal of Experimental Botany* **75**: 5204–5219.

Hu N, Sanderson Bj, Guo M, Feng G, Gambhir D, Hale H, Wang D, Hyden B, Liu J, Smart Lb, *et al.* 2023. Evolution of a ZW sex chromosome system in willows. *Nature communications* **14**: 7144.

Hurst Ld, Pál C, Lercher Mj. **2004**. The evolutionary dynamics of eukaryotic gene order. *Nature reviews. Genetics* **5**: 299–310.

Jay P, Tezenas E, Véber A, Giraud T. **2022**. Sheltering of deleterious mutations explains the stepwise extension of recombination suppression on sex chromosomes and other supergenes. *PLOS Biology* **20**: e3001698.

Jeffreys AJ, May CA. **2004**. Intense and highly localized gene conversion activity in human meiotic crossover hot spots. *Nature Genetics* **36**: 151–156.

Jeffries Dl, Gerchen Jf, Scharmann M, Pannell Jr. **2021**. A neutral model for the loss of recombination on sex chromosomes. *Philosophical transactions of the Royal Society of London. Series B, Biological sciences* **376**: 20200096.

Jousson A, Naciri Y, Christe C, Marazzi B, Stauffer F. **2023**. Not just females and males: Unravelling the complex sex determinism of the hemp palm, Trachycarpus fortunei. *American journal of botany* **110**: e16257.

Käfer J, Bewick A, Andres-Robin A, Lapetoule G, Harkess A, Caïus J, Fogliani B, Gâteblé G, Ralph P, dePamphilis CW, *et al.* 2022. A derived ZW chromosome system in *Amborella trichopoda* , representing the sister lineage to all other extant flowering plants. *New Phytologist* **233**: 1636-1642.

Käfer J. **2022**. How sex chromosomes get trapped into nonrecombination. *PLoS biology* **20**: e3001718.

Käfer J, Lartillot N, Marais GAB, Picard F. **2021**. Detecting sex-linked genes using genotyped individuals sampled in natural populations. *Genetics* **218**: iyab053.

Kellogg EA. **2022**. Genetic control of branching patterns in grass inflorescences. *The Plant Cell* **34**: 2518–2533.

Kopp A. **2012**. Dmrt genes in the development and evolution of sexual dimorphism. *Trends in Genetics* **28**: 175–184.

Krasovec M, Chester M, Ridout K, Filatov D. **2018**. The Mutation Rate and the Age of the Sex Chromosomes in Silene latifolia. *Current Biology* **28**: 1832-1838.e4.

Kurakawa T, Ueda N, Maekawa M, Kobayashi K, Kojima M, Nagato Y, Sakakibara H, Kyozuka J. **2007**. Direct control of shoot meristem activity by a cytokinin-activating enzyme. *Nature* **445**: 652–655.

Lanave C, Preparata G, Sacone C, Serio G. **1984**. A new method for calculating evolutionary substitution rates. *Journal of Molecular Evolution* **20**: 86–93.

Lefouili M, Nam K. **2022**. The evaluation of Bcftools mpileup and GATK HaplotypeCaller for variant calling in non-human species. *Scientific Reports* **12**: 11331.

Leite Montalvão AP, Kersten B, Fladung M, Müller NA. **2021**. The Diversity and Dynamics of Sex Determination in Dioecious Plants. *Frontiers in Plant Science* **11**: 2280.

Lenormand T, Roze D. **2022**. Y recombination arrest and degeneration in the absence of sexual dimorphism. *Science (New York, N.Y.)* **375**: 663–666.

Li H, Durbin R. **2009**. Fast and accurate short read alignment with Burrows-Wheeler transform. *Bioinformatics (Oxford, England)* **25**: 1754–1760.

Li Q, Liu B. **2017**. Genetic regulation of maize flower development and sex determination. *Planta* **245**: 1–14.

Löytynoja A. **2014**. Phylogeny-aware alignment with PRANK. *Methods in molecular biology (Clifton, N.J.)* **1079**: 155–170.

Manichaikul A, Mychaleckyj JC, Rich SS, Daly K, Sale M, Chen W-M. **2010**. Robust relationship inference in genome-wide association studies. *Bioinformatics* **26**: 2867–2873.

Marais Ga, Forrest A, Kamau E, Käfer J, Daubin V, Charlesworth D. **2011**. Multiple nuclear gene phylogenetic analysis of the evolution of dioecy and sex chromosomes in the genus Silene. *PloS one* **6**: e21915.

Martínez-Redondo GI, Barrios-Núñez I, Vázquez-Valls M, Rojas AM, Fernández R. **2024**. Illuminating the functional landscape of the dark proteome across the Animal Tree of Life through natural language processing models. *bioRxiv*: 2024.02.28.582465.

Mascher M, Richmond Ta, Gerhardt Dj, Himmelbach A, Clissold L, Sampath D, Ayling S, Steuernagel B, Pfeifer M, D'Ascenzo M, *et al.* 2013. Barley whole exome capture: a tool for genomic research in the genus Hordeum and beyond. *The Plant journal : for cell and molecular biology* **76**: 494–505.

Massonnet M, Cochetel N, Ricciardi V, Minio A, Figueroa-Balderas R, Londo J, Cantu D. **2024**. Evolutionary conservation of the grape sex-determining region in angiosperms and emergence of dioecy in Vitaceae. *BioRxiv*: 2024.11.10.622717.

Mathew LS, Spannagl M, Al-Malki A, George B, Torres MF, Al-Dous EK, Al-Azwani EK, Hussein E, Mathew S, Mayer KF, *et al.* 2014. A first genetic map of date palm (Phoenix dactylifera) reveals long-range genome structure conservation in the palms. *BMC Genomics* **15**: 285.

Ming R, Bendahmane A, Renner SS. **2011**. Sex Chromosomes in Land Plants. *Annual Review of Plant Biology* **62**: 485–514.

Mitchell Ch, Diggle Pk. **2005**. The evolution of unisexual flowers: morphological and functional convergence results from diverse developmental transitions. *American journal of botany* **92**: 1068-1076.

Morgan EJ, Kaiser-Bunbury CN, Edwards PJ, Scharmann M, Widmer A, Fleischer-Dogley F, Kettle CJ. **2020**. Identification of sex-linked markers in the sexually cryptic coco de mer: are males and females produced in equal proportions? *AoB Plants* **12**: plz079.

Nadot S, Alapetite E, Baker WJ, Tregear JW, Barfod AS. **2016**. The palm family (Arecaceae): a microcosm of sexual system evolution. *Botanical Journal of the Linnean Society* **182**: 376–388.

Niederstätter H, Berger B, Erhart D, Willuweit S, Geppert M, Gassner C, Schennach H, Parson W, Roewer L. **2013**. Multiple recurrent mutations at four human Y-chromosomal single nucleotide polymorphism sites in a 37 bp sequence tract on the ARSDP1 pseudogene. *Forensic science international. Genetics* **7**: 593-600.

O'Meally D, Ezaz T, Georges A, Sarre Sd, Graves Ja. **2012**. Are some chromosomes particularly good at sex? Insights from amniotes. *Chromosome research : an international journal on the molecular, supramolecular and evolutionary aspects of chromosome biology* **20**: 7-19.

Ong A-L, Teh C-K, Mayes S, Massawe F, Appleton DR, Kulaveerasingam H. **2020**. An Improved Oil Palm Genome Assembly as a Valuable Resource for Crop Improvement and Comparative Genomics in the Arecoideae Subfamily. *Plants (Basel, Switzerland)* **9**: 1476.

PALMweb 2025. Palmweb: Palms of the World Online. published on the internet https://palmweb.org/. Accessed 2 February 2025.

Pertea G, Pertea M. **2020**. GFF Utilities: GffRead and GffCompare. *F1000Research* **9**: 304.

Ponnikas S, Sigeman H, Abbott JK, Hansson B. **2018**. Why Do Sex Chromosomes Stop Recombining? *Trends in Genetics* **34**: 492–503.

Prentout D, Stajner N, Cerenak A, Tricou T, Brochier-Armanet C, Jakse J, Käfer J, Marais GAB. **2021**. Plant genera *Cannabis* and *Humulus* share the same pair of well-differentiated sex chromosomes. *New Phytologist* **231**: 1599–1611.

Purcell S, Neale B, Todd-Brown K, Thomas L, Ferreira MAR, Bender D, Maller J, Sklar P, de Bakker PIW, Daly MJ, *et al.* 2007. PLINK: A Tool Set for Whole-Genome Association and Population-Based Linkage Analyses. *American Journal of Human Genetics* **81**: 559.

Quinlan AR, Hall IM. **2010**. BEDTools: a flexible suite of utilities for comparing genomic features. *Bioinformatics* **26**: 841–842.

Rambaut A, Drummond AJ, Xie D, Baele G, Suchard MA. **2018**. Posterior Summarization in Bayesian Phylogenetics Using Tracer 1.7. *Systematic Biology* **67**: 901–904.

Renner SS. **2014**. The relative and absolute frequencies of angiosperm sexual systems: Dioecy, monoecy, gynodioecy, and an updated online database. *American Journal of Botany* **101**: 1588–1596.

Renner SS, Müller NA. **2021**. Plant sex chromosomes defy evolutionary models of expanding recombination suppression and genetic degeneration. *Nature Plants* **7**: 392–402.

Rohland N, Reich D. **2012**. Cost-effective, high-throughput DNA sequencing libraries for multiplexed target capture. *Genome Research* **22**: 939–946.

Rosser ZH, Balaresque P, Jobling MA. **2009**. Gene Conversion between the X Chromosome and the Male-Specific Region of the Y Chromosome at a Translocation Hotspot. *American Journal of Human Genetics* **85**: 130.

Sauquet H, von Balthazar M, Magallón S, Doyle Ja, Endress Pk, Bailes Ej, Barroso de Morais E, Bull-Hereñu K, Carrive L, Chartier M, *et al.* 2017. The ancestral flower of angiosperms and its early diversification. *Nature communications* **8**: 16047.

Sawyer S. **1989**. Statistical tests for detecting gene conversion. *Molecular biology and evolution* **6**: 526–538.

Shumate A, Salzberg SL. **2021**. Liftoff: accurate mapping of gene annotations. *Bioinformatics* **37**: 1639–1643.

Siljak-Yakovlev S, Cerbah M, Sarr A, Benmalek S, Bounaga N, Coba de la Pena T, Brown SC. **1996**. Chromosomal sex determination and heterochromatin structure in date palm. *Sexual Plant Reproduction* **9**: 127–132.

Singh R, Ong-Abdullah M, Low E-TL, Manaf MAA, Rosli R, Nookiah R, Ooi LC-L, Ooi S-E, Chan K-L, Halim MA, *et al.* 2013. Oil palm genome sequence reveals divergence of interfertile species in Old and New worlds. *Nature* **500**: 335–339.

Somaratne Y, Tian Y, Zhang H, Wang M, Huo Y, Cao F, Zhao L, Chen H. **2017**. ABNORMAL POLLEN VACUOLATION1 (APV1) is required for male fertility by contributing to anther cuticle and pollen exine formation in maize. *The Plant journal : for cell and molecular biology* **90**: 96–110.

Tomaszkiewicz M, Medvedev P, Makova Kd. **2017**. Y and W Chromosome Assemblies: Approaches and Discoveries. *Trends in genetics : TIG* **33**: 266–282.

Torres MF, Mathew LS, Ahmed I, Al-Azwani IK, Krueger R, Rivera-Nuñez D, Mohamoud YA, Clark AG, Suhre K, Malek JA. **2018**. Genus-wide sequencing supports a two-locus model for sex-determination in Phoenix. *Nature Communications* **9**: 3969.

Tregear Jw, Richaud F, Collin M, Esbelin J, H P, Cochard B, Nodichao L, Morcillo F, Adam H, Jouannic S. **2022**. Micro-RNA-Regulated SQUAMOSA-PROMOTER BINDING PROTEIN-LIKE (SPL) Gene Expression and Cytokinin Accumulation Distinguish Early-Developing Male and Female Inflorescences in Oil Palm (Elaeis guineensis). *Plants (Basel, Switzerland)* **11**: 685.

Vasimuddin Md, Misra S, Li H, Aluru S. **2019**. Efficient Architecture-Aware Acceleration of BWA-MEM for Multicore Systems. *IEEE International Parallel and Distributed Processing Symposium (IPDPS)*: 314–324.

Xie K, Wu S, Li Z, Zhou Y, Zhang D, Dong Z, An X, Zhu T, Zhang S, Liu S, *et al.* 2018. Map-based cloning and characterization of Zea mays male sterility33 (ZmMs33) gene, encoding a glycerol-3-phosphate acyltransferase. *TAG. Theoretical and applied genetics. Theoretische und angewandte Genetik* **131**: 1363–1378.

Yamaki S, Nagato Y, Kurata N, Nonomura K. **2011**. Ovule is a lateral organ finally differentiated from the terminating floral meristem in rice. *Developmental biology* **351**: 208–216.

Yang Z. **1994a**. Maximum likelihood phylogenetic estimation from DNA sequences with variable rates over sites: Approximate methods. *Journal of Molecular Evolution* **39**: 306–314.

Yang Z. **2007**. PAML 4: Phylogenetic Analysis by Maximum Likelihood. *Molecular Biology and Evolution* **24**: 1586–1591.

Yang X, Wu D, Shi J, He Y, Pinot F, Grausem B, Yin C, Zhu L, Chen M, Luo Z, *et al.* 2014. Rice CYP703A3, a cytochrome P450 hydroxylase, is essential for development of anther cuticle and pollen exine. *Journal of integrative plant biology* **56**: 979–994.

Yang Z. **1993**. Maximum-likelihood estimation of phylogeny from DNA sequences when substitution rates differ over sites. *Molecular biology and evolution* **10**: 1396–1401.

Yang Z. **1994b**. Estimating the pattern of nucleotide substitution. *Journal of molecular evolution* **39**: 105-111.

Yao G, Zhang Y-Q, Barrett C, Xue B, Bellot S, Baker WJ, Ge X-J. **2023**. A plastid phylogenomic framework for the palm family (Arecaceae). *BMC Biology* **21**: 1–15.

Yu G. **2020**. Using ggtree to Visualize Data on Tree-Like Structures. *Current protocols in bioinformatics* **69**: e96.

Zhou G, Yin H, Chen F, Wang Y, Gao Q, Yang F, He C, Zhang L, Wan Y. **2022**. The genome of Areca catechu provides insights into sex determination of monoecious plants. *New Phytologist* **236**: 2327–2343.

Supplementary

Supplementary notes : Detailed target capture protocol.

For each individual, 100 ng of total DNA are sheared using the NEBNext Ultra II FS DNA Modul (New England Biolabs, Ipswich, MA, USA, Part # E7810) by mixing 3.5 µL of NEBNext Ultra II FS Reaction Buffer and 1 µL of NEBNext Ultra II FS Enzyme Mix and an incubation step of 10 min at 37°C. A clean-up step is performed with 1 x volume of Agencourt AMPure XP magnetic beads (Beckman Coulter, Indianapolis, IN, USA, Part # A63881). Fragmented DNA is ligated with 4 pmol of PE-P5 and MPE-P7 adapters. Each PE-P5 and each MPE-P7 adapter carries the same specific hexamer barcode (Rohland & Reich, 2012). Reactions are conducted in 50 µl final volume with 2 unit of T4 DNA ligase (Invitrogen, Thermo Fischer Scientific, Part # 15224025) for 4 hours at 22 °C followed by a heat inactivation step at 65°C for 10 minutes. A clean-up step is performed with 1 x volume of Agencourt AMPure XP magnetic beads. For each individual sample, a pre-hybridization PCR is performed using the KAPA® HiFi HotStart ReadyMix PCR Kit (Roche Diagnostics Indianapolis, IN, USA, Part # KK2602) with 200 nM PreHyb-PE_F (CTTTCCCTACACGACGCTCTTC) and 200 nM PreHyb-MPE_R (TGACTGGAGTTCAGACGTGTG) primers in a final volume of 100µl. Thermocycling parameters were 2 minutes at 98°C, followed by 12 cycles of 20 seconds at 98°C; 45 seconds at 55°C and 30 seconds at 72°C, with a final elongation of 10 minutes at 72°C. A clean-up step is performed with 1 x volume Agencourt AMPure XP magnetic beads. Amplified DNA is individually controlled (sizing and estimation of the concentration) by electrophoresis on a AATI Fragment Analyzer™ (Advanced Analytical Technologies, Ankeny, IA, USA) device with the DNF-474 High Sensitivity Fragment Analysis Kit. Until 24 samples (corresponding to 24 hexamer barcodes on the PE-P5 and PE-P7 adapter) are pooled. A clean-up step is performed with 1 x volume of Agencourt AMPure XP magnetic beads.

Enrichment and capture by hybridization followed the Standard Protocol, with a hybridization and washing temperature of 65°C, following the indications of the User Manual of the myBaits Hybridization Capture for Targeted NGS, Custom DNA-Seq (protocol version 4.01 (http://www.mycroarray.com)). An on-beads PCR amplification is undertaken to enrich library fragments, extend the adapter sequence and incorporate an index to the P7 adapter. The PCR reaction is

34

using the KAPA® HiFi HotStart ReadyMix PCR Kit (KAPABiosystems, Boston, MA, Part # KR0370) in a final volume of 50 µl with:

- 15 pmol of SOL-PE-PCR_F primer (Mascher M *et al.*, 2013)

  aatgatacggcgaccaccgagatctacactctttccctacacgacgctcttc

- 15 pmol of SOL-MPE-INDX_R indexed primers

  CAAGCAGAAGACGGCATACGAGATXXXXXXGTGACTGGAGTTCAGACGTGT

This primer carries 6 bases of the official TruSeq Illumina Index. Thermocycling parameters were 2 minutes at 98°C, followed by 18 cycles of 20 seconds at 98°C; 30 seconds at 62°C and 30 seconds at 72°C, with a final elongation of 5 minutes at 72°C. The reaction volume is 50 µL. A clean-up step is performed with 1.3 x volume Agencourt AMPure XP magnetic beads. The elution volume is 20 µL. Indexed libraries are individually controlled (sizing and estimation of the concentration) by electrophoresis on an AATI Fragment Analyzer™ device with the DNF-474 High Sensitivity Fragment Analysis Kit. The different indexed libraries, corresponding to all the captured barcoded DNA samples, are equally mixed. The final pooled library is quantified by qPCR with the KAPA Library Quantification Kit (Part # KK4824).

Table S1. Classification of sex-linked genes according to SDpop output and X-Y synonymous divergence (dS).

Gene category [1]	SDpop posterior score	dS
High-confidence sex-linked (HCSL)	XY score > 0.8	> 0.0021 *P. dactylifera* > 0.0011 *K. elegans*
Probably sex-linked (PSL)	XY score > 0.8	< 0.0021 *P. dactylifera* < 0.0011 *K. elegans*
	0.5 < XY score < 0.8	
Not sex-linked / Autosomal	Autosomal score > 0.8	
Inconclusive	Other scores	
NA	No data	

[1] only applies to genes with more than 10 individuals genotyped on average; other genes are considered "inconclusive"

Table S2. Reads mapping of the samples in the *P. dactylifera* WGS dataset.

Sample name	Reads (R1 + R2)	Mapped properly paired	Discarded[1]
SRR10121061	69906798	93.41%	Yes
SRR10121067	79422680	94.90%	Yes
SRR10121077	94044556	95.49%	No
SRR10121086	70564142	94.67%	Yes
SRR10121091	76352168	92.67%	No
SRR10121093	99377344	93.34%	No
SRR10121095	94123466	95.07%	No
SRR10121106	94660272	96.39%	No
SRR10121107	61350290	92.63%	No
SRR10121111	81614162	96.86%	No
SRR10121117	74139608	96.28%	Yes
SRR10121120	87950120	93.51%	No
SRR10121126	78984780	95.37%	No
SRR10121130	60753842	92.48%	No
SRR10121134	92117304	94.42%	No
SRR10121138	89963210	93.65%	No
SRR10121146	88845434	93.90%	No
SRR10121160	69178418	93.86%	No
SRR10121164	77056038	94.57%	No
SRR10121166	88559374	93.80%	No
SRR10121171	88773146	94.72%	No
SRR10121175	82661366	94.40%	No
SRR10121177	80185434	93.98%	No
SRR10121178	69218370	93.77%	No
SRR10121179	81745170	94.27%	Yes
SRR10121180	77771724	92.10%	No
SRR10121181	85821024	93.58%	No
SRR10121182	110764132	94.73%	No
SRR10121183	98825142	94.39%	No
SRR10121184	77905032	94.70%	No
SRR10121185	81762922	94.44%	No
SRR10121186	96158186	94.68%	Yes

[1] Related individuals (see Figure S2-A) that were discarded from the analysis are indicated by a “Yes”.

Table S3. Reads mapping and relatedness of the target capture sequences of SexPhoenix (SP) and PalmExons (PE) datasets.

Sample	Species	Reads (R1 + R2)		Mapped properly paired		discarded[1]
		SP	PE	SP	PE	
Pz187-F	*P. dactylifera*	4377416	18632428	99.67%	99.84%	No
Pz188-F	*P. dactylifera*	5008768	18696304	99.61%	99.85%	No
Pz189-F	*P. dactylifera*	2483626	9135350	99.49%	99.75%	No
Pz190-F	*P. dactylifera*	4385870	17747354	99.65%	99.83%	No
Pz191-F	*P. dactylifera*	2939824	10817454	99.62%	99.76%	No
Pz192-F	*P. dactylifera*	3127450	10421980	99.47%	99.41%	No
Pz193-F	*P. dactylifera*	1985378	6219258	99.51%	99.76%	No
Pz194-F	*P. dactylifera*	3061202	11576270	99.54%	99.63%	No
Pz195-F	*P. dactylifera*	2594946	9306702	99.53%	99.63%	No
Pz196-M	*P. dactylifera*	2627820	10596866	99.47%	99.69%	No
Pz197-M	*P. dactylifera*	3694942	16134226	99.51%	99.76%	Yes
Pz198-M	*P. dactylifera*	2281358	9850922	98.30%	96.05%	No
Pz199-M	*P. dactylifera*	2078630	9343366	99.49%	99.77%	No
Pz200-M	*P. dactylifera*	4513112	22881886	99.41%	99.29%	No
Pz201-M	*P. dactylifera*	2016912	11571982	99.44%	99.73%	No
Pz202-M	*P. dactylifera*	1772086	7567128	99.45%	99.70%	No
Pz203-M	*P. dactylifera*	1941712	10554778	99.45%	99.69%	No
Pz204-M	*P. dactylifera*	3704796	20085258	99.55%	99.83%	No
Pz205-M	*P. dactylifera*	3084618	14996024	99.57%	99.79%	No
Pz021-F	*K. elegans*	666270	16383618	84.20%	99.24%	No
Pz022-F	*K. elegans*	752908	17161294	83.45%	99.21%	No
Pz023-F	*K. elegans*	771894	17218782	82.95%	99.17%	No
Pz024-F	*K. elegans*	738372	15364196	83.78%	99.09%	No
Pz025-F	*K. elegans*	874352	19668318	83.90%	99.32%	No
Pz026-F	*K. elegans*	603370	13660796	83.50%	99.17%	No
Pz027-F	*K. elegans*	576916	13522682	84.68%	99.16%	No
Pz028-F	*K. elegans*	752862	18841052	85.51%	99.24%	No
Pz029-F	*K. elegans*	926680	24343416	85.12%	99.40%	No
Pz030-F	*K. elegans*	733968	17460034	84.45%	99.28%	No
Pz031-M	*K. elegans*	789534	18569286	85.17%	99.28%	No
Pz032-M	*K. elegans*	439660	9782804	83.12%	99.23%	No
Pz033-M	*K. elegans*	677530	15510204	84.48%	99.42%	No
Pz034-M	*K. elegans*	500752	11488268	83.08%	98.93%	No
Pz035-M	*K. elegans*	709868	17164758	85.20%	99.27%	No
Pz036-M	*K. elegans*	575470	12718802	83.73%	99.17%	No
Pz037-M	*K. elegans*	623986	13381650	85.05%	98.97%	No
Pz038-M	*K. elegans*	691268	15951318	83.54%	99.24%	No
Pz039-M	*K. elegans*	942786	21623126	84.48%	99.29%	No
Pz040-M	*K. elegans*	756512	18298996	85.16%	99.39%	No
Pz269-F	*K. elegans*	578186	12884964	83.44%	98.83%	No
Pz270-H	*K. elegans*	595258	14863394	83.04%	99.06%	Yes

Pz271-M	*K. elegans*	755654	19055042	84.54%	99.39%	No
Pz272-F	*K. elegans*	508120	11612810	81.86%	99.03%	No
Pz273-F	*K. elegans*	1014112	26035728	82.67%	99.10%	No
Pz274-F	*K. elegans*	607980	12829890	82.60%	99.20%	No

[1] Related individuals that were discarded from the analysis are indicated by a “Yes”.

Table S4. Read depth and coverage of the DPV01 genome protein-coding genes by our different datasets.

	P. dactylifera			K. elegans	
	WGS[1]	SP[2]	PE[3]	SP[2]	PE[3]
DPV01 genes covered (%)[4]	97.61	1.6	77.06	2.54	58.31
Median covered length (%)[5]	99.65	74.80	48.30	53.80	43.30
[1st - 3rd quartile] (%)	[92.25 - 1]	[48.29 – 94.50]	[33.15 – 66.74]	[23.23 – 87.14]	[29.15 – 59.94]
Median depth per base (females)[6]	11.03	39.01	22.43	19.89	32.50
[1st - 3rd quartile]	[10.07 – 11.74]	[11.62 – 93.24]	[8.51 – 48.42]	[1.86 – 82.25]	[9.50 – 87.91]
Median depth per base (males)[6]	11.76	36.07	19.36	18.93	31.18
[1st - 3rd quartile]	[10.85 – 12.40]	[15.01 – 80.80]	[7.70 – 40.75]	[1.88 – 78.84]	[9.10 – 84.67]
Number of variant positions analyzed	466719	4693	180035	8395	161384

[1] Whole Genome Sequencing (WGS)
[2] SexPhoenix capture kit (SP)
[3] PalmExons capture kit (PE)
[4] Percentage of protein coding genes covered from the DPV01 P. dactylifera genome annotation.
[5] Median, first and third quartile of the proportion of the total gene length covered over 10X for WGS and over 7X for SP and PE.
[6] Median, first and third quartile of the mean depth of coverage per base per gene.

Table S5. Summary of SDpop model analysis.

model[1]	BIC[1]	autosomal[2]	haploid[2]	paralog[2]	hemizygote[2]	gametolog[2]
Phoenix dactylifera Whole Genome Sequencing						
XY	**11064321.61**	0.9124	0.0019	0.0791	0.0042	0.0023
ZW	11068885.09	0.9182	0.0022	0.0791	0.0001	0.0004
No sex chromosomes	11068908.67	0.9186	0.0022	0.0792		
Phoenix dactylifera SexPhoenix						
XY	**85066.94**	0.8375	0.0029	0.0403	0.0000	0.1193
ZW	89224.73	0.8881	0.0011	0.0400	0.0707	0.0000
No sex chromosomes	89646.72	0.9572	0.0034	0.0403		
Phoenix dactylifera PalmExons						
XY	**2839713.34**	0.9537	0.0047	0.0387	0.0001	0.0028
ZW	2841129.27	0.9548	0.0046	0.0388	0.0018	0.0000
No sex chromosomes	2841134.61	0.9566	0.0047	0.0388		
Kerriodoxa elegans SexPhoenix						
XY	**113544.76**	0.7420	0.0016	0.1208	0.0000	0.1356
ZW	123130.07	0.8010	0.0009	0.1212	0.0419	0.0349
No sex chromosomes	124038.66	0.8766	0.0014	0.1221		
Kerriodoxa elegans PalmExons						
XY	**2642686.41**	0.6481	0.0031	0.3408	0.0003	0.0077
ZW	2649700.34	0.6558	0.0031	0.3409	0.0000	0.0001
No sex chromosomes	2649680.07	0.6560	0.0031	0.3409		

[1] For *K. elegans*, all SDpop models were run to test for the presence of XY or ZW chromosomes; the model with the lowest Bayesian Information Criterion (BIC), i.e. the most likely, is printed in bold.

[2] The optimized proportion of SNPs for each segregation type is given.

41

Table S6: Summary of the number of genes in Whole Genome Sequencing (WGS) and PalmExons capture (PE) datasets and position of sex-linked genes.

Number of genes	**Pd[1] WGS**	**Pd PE**	**Ke[1] PE**
Total (in analysis)	25 100	19 889	15 051
High-confidence or probably sex-linked[3]	87	68	89
P. dactylifera PDMBC4 genome Chr12:9.4-12.4Mb[4]	22	12	16
P. dactylifera PDMBC4 genome unplaced scaffold[4]	39	25	36
E. guineensis[5] EGPMv6 genome Chr10:43-46.1Mb[4]	52	29	55
E. guineensis EGPMv6 genome unplaced scaffold[4]	0	0	2

[1] *Phoenix dactylifera*
[2] *Kerriodoxa elegans*
[3] see Material and Methods
[4] Among High-confidence or probably sex-linked
[5] *Elaeis guineensis*

42

Table S7. Classification of protein-coding genes in the region of *E. guineensis* homologous with the sex-linked region in *P. dactylifera* and *K. elegans*.

Category[1]	*Phoenix dactylifera*[2]	*Kerriodoxa elegans*[2]	Common[2,3]
High-confidence sex-linked	31	53	19
Probably sex-linked	25	9	22
Not sex-linked	17	0	0
NA	0	18	18
Inconclusive	24	17	31
Contrasting[3]			7

[1] For the definition of these categories, see Table S1.

[2] Gene counts correspond to the *Elaeis guineensis* protein-coding genes present in the region homologous to the *P. dactylifera* and *K. elegans* sex-linked region that had an annotation in *P. dactylifera* (DPV01, Al-Mssallem *et al.*, 2013). Two Y-specific genes were added from the male P. dactylifera annotation (Hazzouri et al., 2019).

[3] For each gene, the category assigned under “common” is the most conservative among the two species, i.e. a gene “probably sex-linked” in one species and “high-confidence sex-linked” in the other is considered “probably sex-linked” in both. Genes considered as “contrasting” were sex-linked (either high-confidence or probably) in one species and autosomal in the other.

43

Table S8. XY sequences for which gene conversion was detected.

Gene	XY paired sequences[1]	Simulated p-value[2]	KA p-value[2]	start position[3]	end position[3]
LOC103695972	*P. dactylifera* WGS[4]	0.01	0.03	1013	1214
LOC103695972	*P. dactylifera* SP[5]	0.01	0.03	1013	1214
LOC103698366	*P. dactylifera* WGS	0.02	0.09	73	716
LOC103698366	*P. dactylifera* SP	0.01	0.05	73	716
LOC103716262	*K. elegans* SP	0.01	0.08	250	699
LOC103723089	*K. elegans* SP	0.02	0.14	448	1061
LOC103724019	*P. dactylifera* WGS	0.02	0.08	3299	4064
LOC103724019	*P. dactylifera* SP	0.03	0.11	3299	4064
LOC103723285	*K. elegans* SP	0.00	0.02	686	824

[1] Dataset of gene sequences where gene conversion was detected between the X and Y copies.
[2] KA p-values are more conservative and less accurate than simulated p-values. Only one was required to be below 0.05 to be included.
[3] Start and end position of the alignment which underwent gene conversion.
[4] Whole Genome Sequencing (WGS) data.
[5] SexPhoenix (SP) target capture data.

44

Table S9. Synonymous divergence (dS) between *Elaeis guineensis* and *Phoenix dactylifera* for ten random autosomal single copy orthologs.

***Elaeis guineensis* gene**	***Phoenix dactylifera* gene**	**Gene function**	**dS**
LOC105059023	LOC103698418	DNA repair protein RAD51 homolog 3	0.18
LOC105056566	LOC103703289	thyroid adenoma-associated protein homolog	0.12
LOC105056732	LOC103705344	pentatricopeptide repeat-containing protein OGR1	0.23
LOC105057008	LOC103706629	nudix hydrolase 9	0.15
LOC105036130	LOC103708307	FT-interacting protein 7	0.30
LOC105049520	LOC103711984	chloride channel protein CLC-e	0.12
LOC105052889	LOC103713882	tetratricopeptide repeat protein SKI3	0.10
LOC105047177	LOC103714988	anaphase-promoting complex subunit 10	0.15
LOC105057153	LOC103720210	uncharacterized	0.22
LOC105057944	LOC103720756	uncharacterized	0.06

45

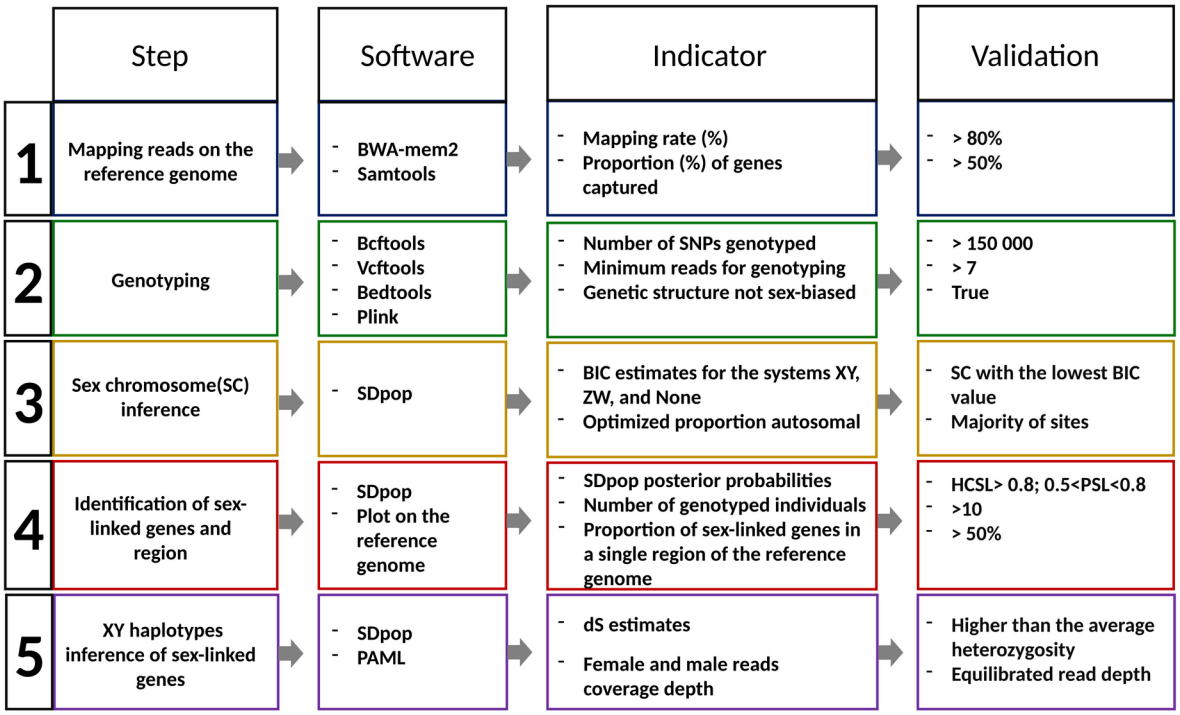

Figure S1. Strategy summary. Here are the main steps of our analysis with the softwares, their variables and threshold values used for step validation.

46

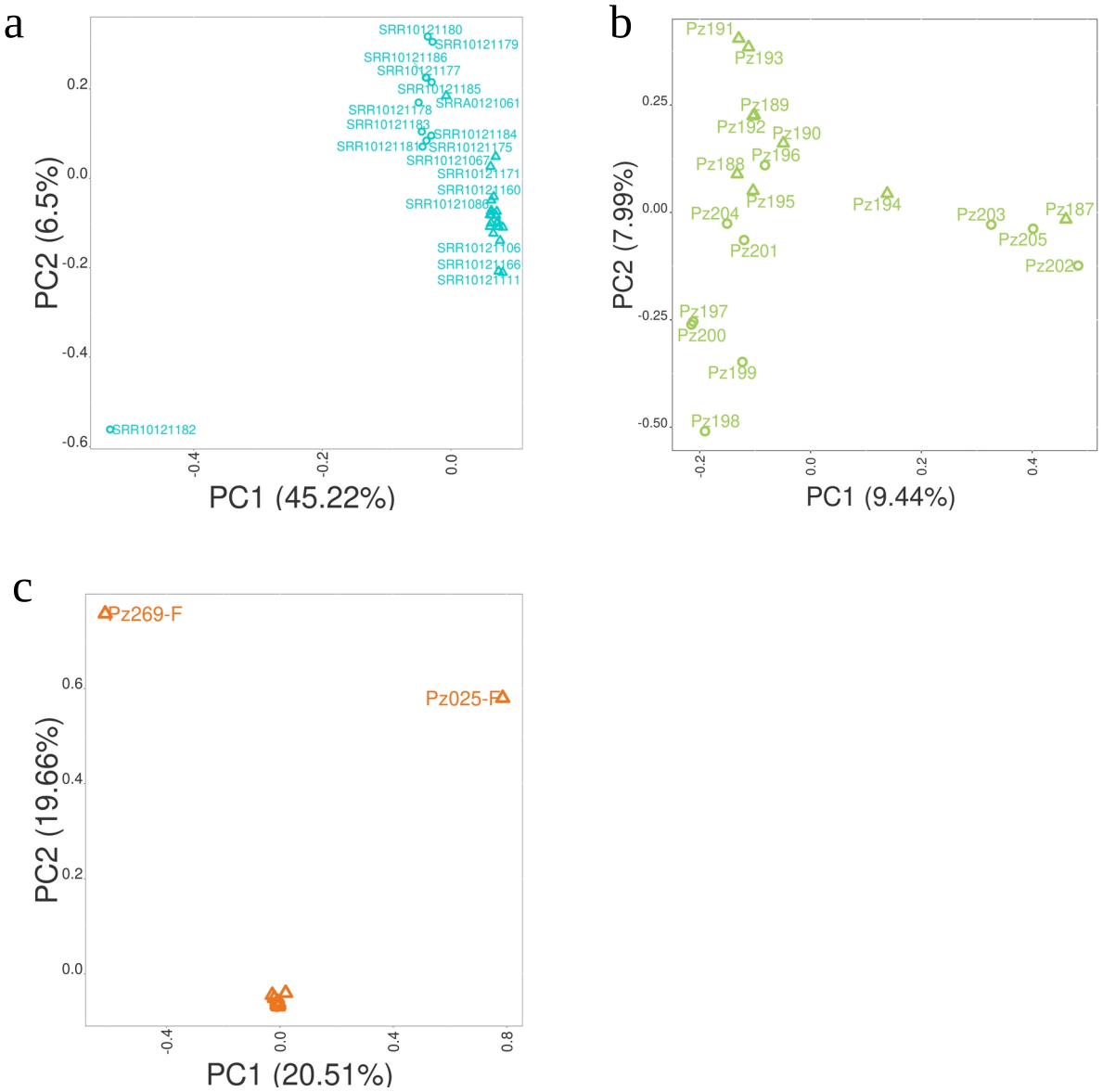

Figure S2. PCA of the genetic variation of studied populations. Females are represented by triangles, males by circles, one ambiguous *K. elegans* individual by a square. **(a)** PCA of the genetic variation of the *P. dactylifera* whole genome individuals. **(b)** PCA of the genetic variation captured with PalmExons kit among the *P. dactylifera* individuals. **(c)** PCA of the genetic variation captured with PalmExons kit among the *K. elegans* individuals.

47

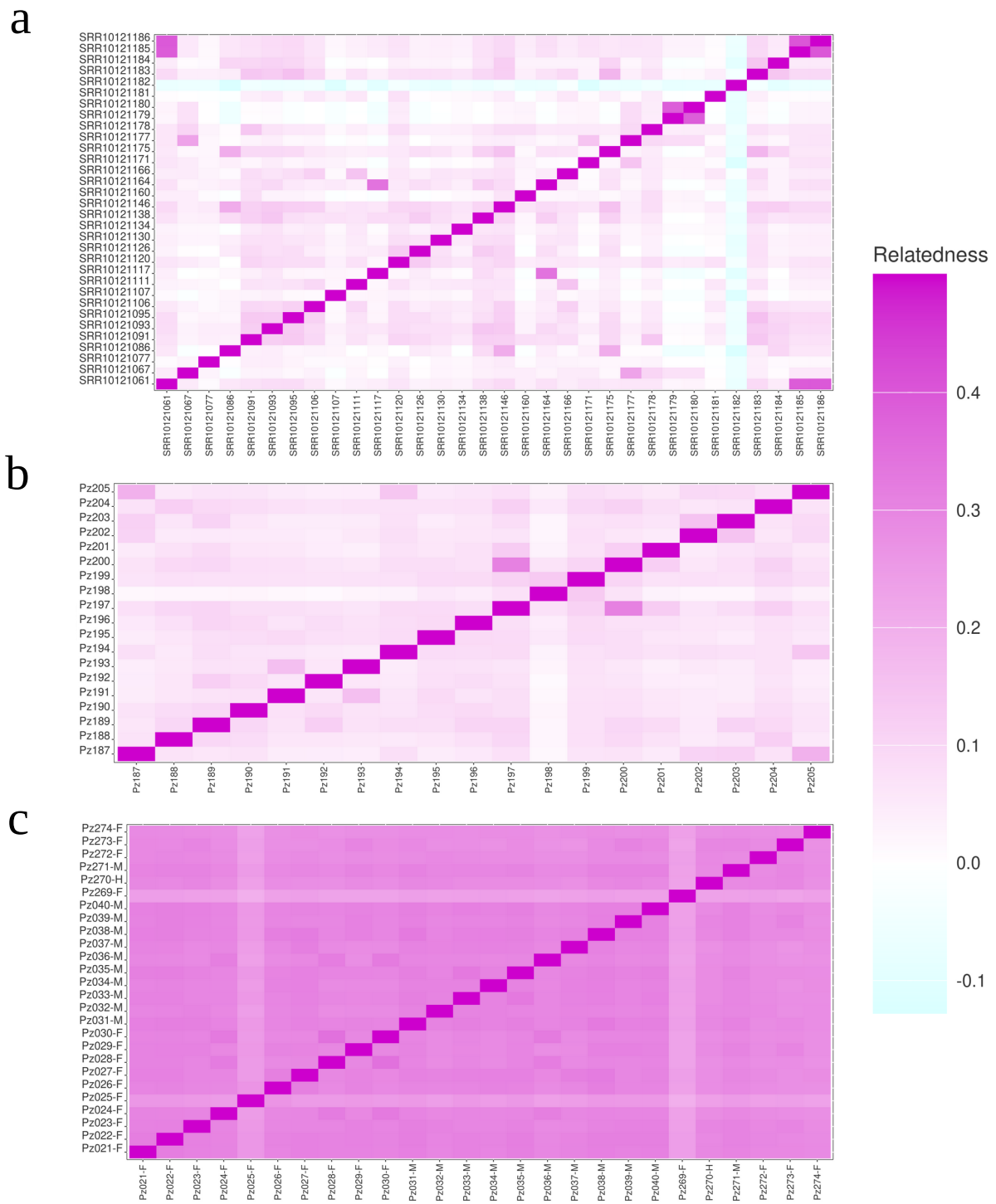

Figure S3. Heatmap of estimated relatedness between individuals. A relatedness of 0 is represented by a white square and indicates unrelated individuals from the same population. A relatedness of 0.5 (the maximum value) is represented with a magenta square and is characteristic of clones. A cyan square indicates negative relatedness as one would expect between different populations. Gradients between these colors represent intermediate values. **(a)** Heatmap of the relatedness between *P. dactylifera* whole genome individuals. **(b)** Heatmap of

48

the relatedness between *P. dactylifera* individuals in the data captured with PalmExons kit. **(c)** Heatmap of the relatedness between *K. elegans* individuals in the data captured with PalmExons kit.

49

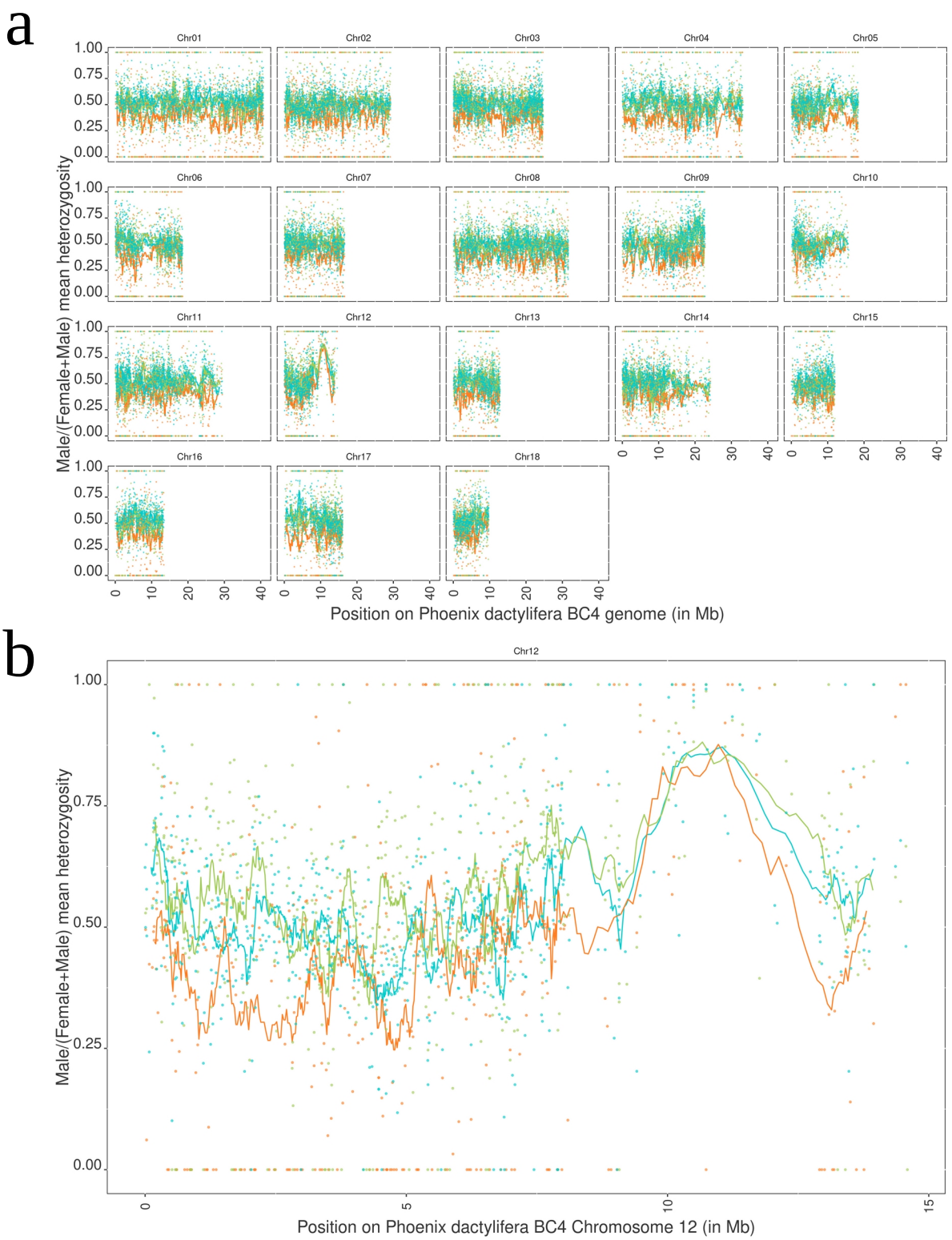

Figure S4. Male mean heterozygosity proportion per gene mapped on PDMBC4 genome of *P. dactylifera.* Male (M) and female (F) mean heterozygosity rate per gene on all genotyped positions were calculated. Genes without heterozygosity were removed. Then, the ratio of male

50

mean heterozygosity over female and male mean heterozygosity was calculated : M/(M+F). **(a)** Male mean heterozygosity proportion per gene is represented on the chromosomes of the *Phoenix dactylifera* PDMBC4 genome. **(b)** Male mean heterozygosity proportion per gene is represented on the 12th chromosome of the PDMBC4 genome. Each line represents the rolling mean over 15 genes colored according to the species and dataset : *P. dactylifera* Whole Genome Sequencing (WGS; cyan), PalmExons capture sequence for *P. dactylifera* (green) and *K. elegans* (orange).

51

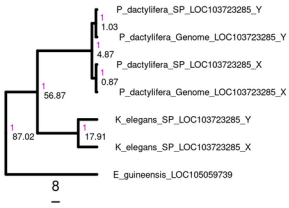
P_dactylifera_SP_LOC103723285_Y
P_dactylifera_Genome_LOC103723285_Y
P_dactylifera_SP_LOC103723285_X
P_dactylifera_Genome_LOC103723285_X
K_elegans_SP_LOC103723285_Y
K_elegans_SP_LOC103723285_X
E_guineensis_LOC105059739
1.03
4.87
0.87
56.87
87.02
17.91
8

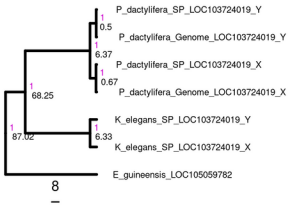
P_dactylifera_SP_LOC103724019_Y
P_dactylifera_Genome_LOC103724019_Y
P_dactylifera_SP_LOC103724019_X
P_dactylifera_Genome_LOC103724019_X
K_elegans_SP_LOC103724019_Y
K_elegans_SP_LOC103724019_X
E_guineensis_LOC105059782
0.5
6.37
0.67
68.25
87.02
6.33
8

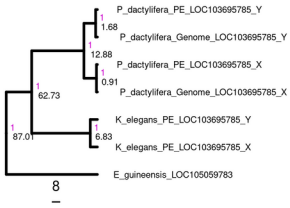
P_dactylifera_PE_LOC103695785_Y
P_dactylifera_Genome_LOC103695785_Y
P_dactylifera_PE_LOC103695785_X
P_dactylifera_Genome_LOC103695785_X
K_elegans_PE_LOC103695785_Y
K_elegans_PE_LOC103695785_X
E_guineensis_LOC105059783
1.68
12.88
0.91
62.73
87.01
6.83
8

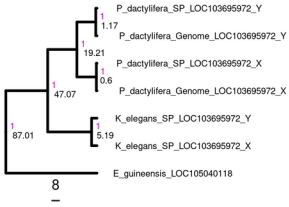
P_dactylifera_SP_LOC103695972_Y
P_dactylifera_Genome_LOC103695972_Y
P_dactylifera_SP_LOC103695972_X
P_dactylifera_Genome_LOC103695972_X
K_elegans_SP_LOC103695972_Y
K_elegans_SP_LOC103695972_X
E_guineensis_LOC105040118
1.17
19.21
0.6
47.07
87.01
5.19
8

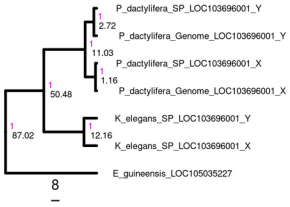
P_dactylifera_SP_LOC103696001_Y
P_dactylifera_Genome_LOC103696001_Y
P_dactylifera_SP_LOC103696001_X
P_dactylifera_Genome_LOC103696001_X
K_elegans_SP_LOC103696001_Y
K_elegans_SP_LOC103696001_X
E_guineensis_LOC105035227
2.72
11.03
1.16
50.48
87.02
12.16
8

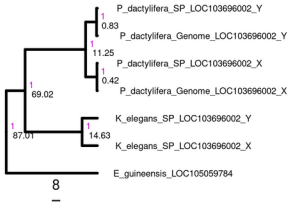
P_dactylifera_SP_LOC103696002_Y
P_dactylifera_Genome_LOC103696002_Y
P_dactylifera_SP_LOC103696002_X
P_dactylifera_Genome_LOC103696002_X
K_elegans_SP_LOC103696002_Y
K_elegans_SP_LOC103696002_X
E_guineensis_LOC105059784
0.83
11.25
0.42
69.02
87.01
14.63
8

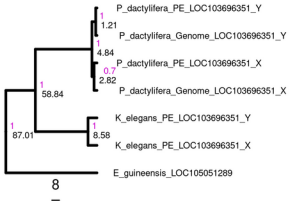
P_dactylifera_PE_LOC103696351_Y
P_dactylifera_Genome_LOC103696351_Y
P_dactylifera_PE_LOC103696351_X
P_dactylifera_Genome_LOC103696351_X
K_elegans_PE_LOC103696351_Y
K_elegans_PE_LOC103696351_X
E_guineensis_LOC105051289
1.21
4.84
0.7
2.82
58.84
87.01
8.58
8

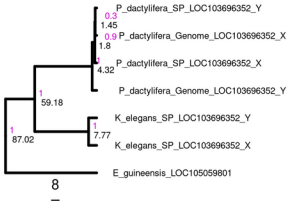
P_dactylifera_SP_LOC103696352_Y
P_dactylifera_Genome_LOC103696352_X
P_dactylifera_SP_LOC103696352_X
P_dactylifera_Genome_LOC103696352_Y
K_elegans_SP_LOC103696352_Y
K_elegans_SP_LOC103696352_X
E_guineensis_LOC105059801
0.3
1.45
0.9
1.8
4.32
59.18
87.02
7.77
8

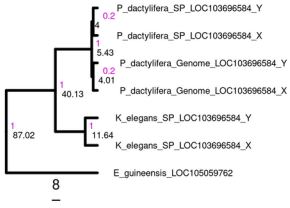
P_dactylifera_SP_LOC103696584_Y
P_dactylifera_SP_LOC103696584_X
P_dactylifera_Genome_LOC103696584_Y
P_dactylifera_Genome_LOC103696584_X
K_elegans_SP_LOC103696584_Y
K_elegans_SP_LOC103696584_X
E_guineensis_LOC105059762
0.2
5.43
0.2
4.01
40.13
87.02
11.64
8

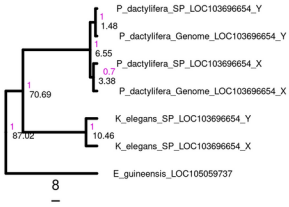
P_dactylifera_SP_LOC103696654_Y
P_dactylifera_Genome_LOC103696654_Y
P_dactylifera_SP_LOC103696654_X
P_dactylifera_Genome_LOC103696654_X
K_elegans_SP_LOC103696654_Y
K_elegans_SP_LOC103696654_X
E_guineensis_LOC105059737
1.48
6.55
0.7
3.38
70.69
87.02
10.46
8

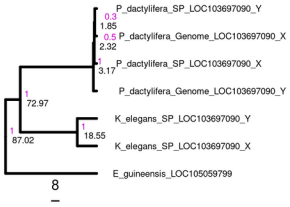
P_dactylifera_SP_LOC103697090_Y
P_dactylifera_Genome_LOC103697090_X
P_dactylifera_SP_LOC103697090_X
P_dactylifera_Genome_LOC103697090_Y
K_elegans_SP_LOC103697090_Y
K_elegans_SP_LOC103697090_X
E_guineensis_LOC105059799
0.3
1.85
0.5
2.32
3.17
72.97
87.02
18.55
8

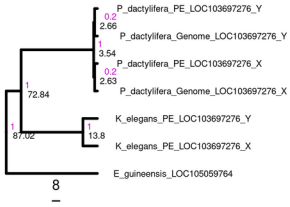
P_dactylifera_PE_LOC103697276_Y
P_dactylifera_Genome_LOC103697276_Y
P_dactylifera_PE_LOC103697276_X
P_dactylifera_Genome_LOC103697276_X
K_elegans_PE_LOC103697276_Y
K_elegans_PE_LOC103697276_X
E_guineensis_LOC105059764
0.2
2.66
3.54
0.2
2.63
72.84
87.02
13.8
8

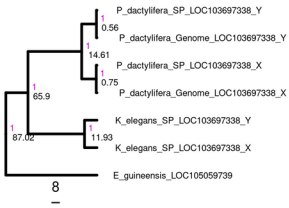
P_dactylifera_SP_LOC103697338_Y
P_dactylifera_Genome_LOC103697338_Y
P_dactylifera_SP_LOC103697338_X
P_dactylifera_Genome_LOC103697338_X
K_elegans_SP_LOC103697338_Y
K_elegans_SP_LOC103697338_X
E_guineensis_LOC105059739
0.56
14.61
0.75
65.9
87.02
11.93
8

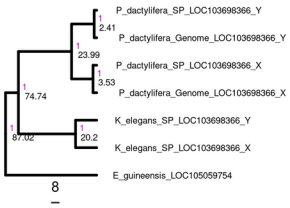
P_dactylifera_SP_LOC103698366_Y
P_dactylifera_Genome_LOC103698366_Y
P_dactylifera_SP_LOC103698366_X
P_dactylifera_Genome_LOC103698366_X
K_elegans_SP_LOC103698366_Y
K_elegans_SP_LOC103698366_X
E_guineensis_LOC105059754
2.41
23.99
3.53
74.74
87.02
20.2
8

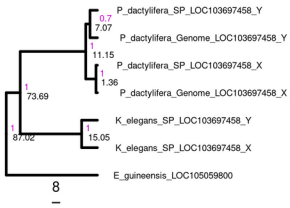
P_dactylifera_SP_LOC103697458_Y
P_dactylifera_Genome_LOC103697458_Y
P_dactylifera_SP_LOC103697458_X
P_dactylifera_Genome_LOC103697458_X
K_elegans_SP_LOC103697458_Y
K_elegans_SP_LOC103697458_X
E_guineensis_LOC105059800
0.7
7.07
11.15
1.36
73.69
87.02
15.05
8

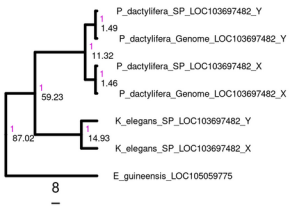
P_dactylifera_SP_LOC103697482_Y
P_dactylifera_Genome_LOC103697482_Y
P_dactylifera_SP_LOC103697482_X
P_dactylifera_Genome_LOC103697482_X
K_elegans_SP_LOC103697482_Y
K_elegans_SP_LOC103697482_X
E_guineensis_LOC105059775
1.49
11.32
1.46
59.23
87.02
14.93
8

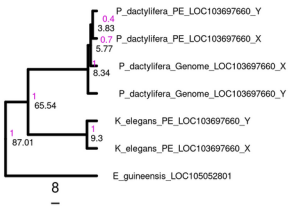
P_dactylifera_PE_LOC103697660_Y
P_dactylifera_PE_LOC103697660_X
P_dactylifera_Genome_LOC103697660_X
P_dactylifera_Genome_LOC103697660_Y
K_elegans_PE_LOC103697660_Y
K_elegans_PE_LOC103697660_X
E_guineensis_LOC105052801
0.4
3.83
0.7
5.77
8.34
65.54
87.01
9.3
8

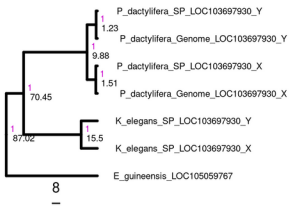
P_dactylifera_SP_LOC103697930_Y
P_dactylifera_Genome_LOC103697930_Y
P_dactylifera_SP_LOC103697930_X
P_dactylifera_Genome_LOC103697930_X
K_elegans_SP_LOC103697930_Y
K_elegans_SP_LOC103697930_X
E_guineensis_LOC105059767
1.23
9.88
1.51
70.45
87.02
15.5
8

52

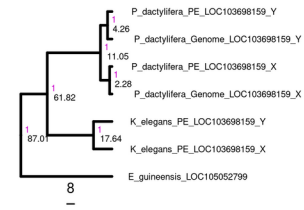
P_dactylifera_PE_LOC103698159_Y
P_dactylifera_Genome_LOC103698159_Y
P_dactylifera_PE_LOC103698159_X
P_dactylifera_Genome_LOC103698159_X
K_elegans_PE_LOC103698159_Y
K_elegans_PE_LOC103698159_X
E_guineensis_LOC105052799
4.26
11.05
2.28
61.82
87.01
17.64
8

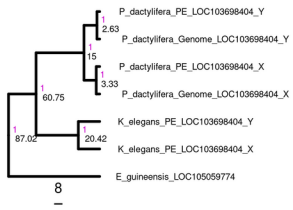
P_dactylifera_PE_LOC103698404_Y
P_dactylifera_Genome_LOC103698404_Y
P_dactylifera_PE_LOC103698404_X
P_dactylifera_Genome_LOC103698404_X
K_elegans_PE_LOC103698404_Y
K_elegans_PE_LOC103698404_X
E_guineensis_LOC105059774
2.63
15
3.33
60.75
87.02
20.42
8

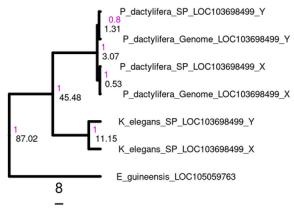
P_dactylifera_SP_LOC103698499_Y
P_dactylifera_Genome_LOC103698499_Y
P_dactylifera_SP_LOC103698499_X
P_dactylifera_Genome_LOC103698499_X
K_elegans_SP_LOC103698499_Y
K_elegans_SP_LOC103698499_X
E_guineensis_LOC105059763
0.8
1.31
3.07
0.53
45.48
87.02
11.15
8

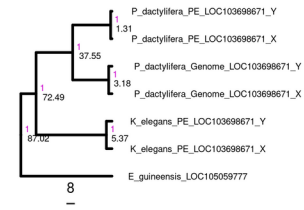
P_dactylifera_PE_LOC103698671_Y
P_dactylifera_PE_LOC103698671_X
P_dactylifera_Genome_LOC103698671_Y
P_dactylifera_Genome_LOC103698671_X
K_elegans_PE_LOC103698671_Y
K_elegans_PE_LOC103698671_X
E_guineensis_LOC105059777
1.31
37.55
3.18
72.49
87.02
5.37
8

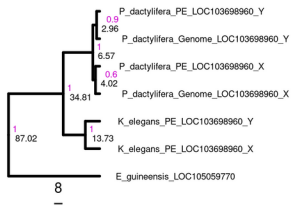
P_dactylifera_PE_LOC103698960_Y
P_dactylifera_Genome_LOC103698960_Y
P_dactylifera_PE_LOC103698960_X
P_dactylifera_Genome_LOC103698960_X
K_elegans_PE_LOC103698960_Y
K_elegans_PE_LOC103698960_X
E_guineensis_LOC105059770
0.9
2.96
6.57
0.6
4.02
34.81
87.02
13.73
8

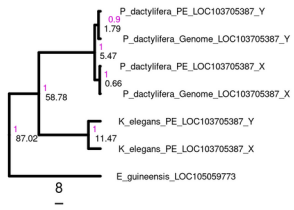
P_dactylifera_PE_LOC103705387_Y
P_dactylifera_Genome_LOC103705387_Y
P_dactylifera_PE_LOC103705387_X
P_dactylifera_Genome_LOC103705387_X
K_elegans_PE_LOC103705387_Y
K_elegans_PE_LOC103705387_X
E_guineensis_LOC105059773
0.9
1.79
5.47
0.66
58.78
87.02
11.47
8

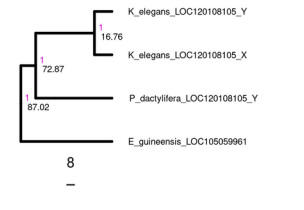
K_elegans_LOC120108105_Y
K_elegans_LOC120108105_X
P_dactylifera_LOC120108105_Y
E_guineensis_LOC105059961
16.76
72.87
87.02
8

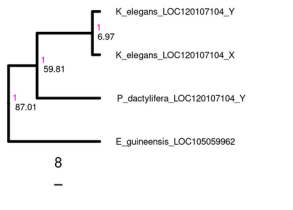
K_elegans_LOC120107104_Y
K_elegans_LOC120107104_X
P_dactylifera_LOC120107104_Y
E_guineensis_LOC105059962
6.97
59.81
87.01
8

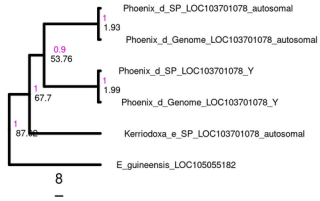
Phoenix_d_SP_LOC103701078_autosomal
Phoenix_d_Genome_LOC103701078_autosomal
Phoenix_d_SP_LOC103701078_Y
Phoenix_d_Genome_LOC103701078_Y
Kerriodoxa_e_SP_LOC103701078_autosomal
E_guineensis_LOC105055182
1.93
0.9
53.76
1.99
67.7
8

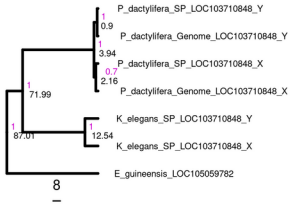
P_dactylifera_SP_LOC103710848_Y
P_dactylifera_Genome_LOC103710848_Y
P_dactylifera_SP_LOC103710848_X
P_dactylifera_Genome_LOC103710848_X
K_elegans_SP_LOC103710848_Y
K_elegans_SP_LOC103710848_X
E_guineensis_LOC105059782
0.9
3.94
0.7
2.16
71.99
87.01
12.54
8

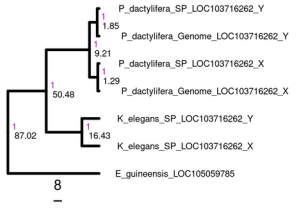
P_dactylifera_SP_LOC103716262_Y
P_dactylifera_Genome_LOC103716262_Y
P_dactylifera_SP_LOC103716262_X
P_dactylifera_Genome_LOC103716262_X
K_elegans_SP_LOC103716262_Y
K_elegans_SP_LOC103716262_X
E_guineensis_LOC105059785
1.85
9.21
1.29
50.48
87.02
16.43
8

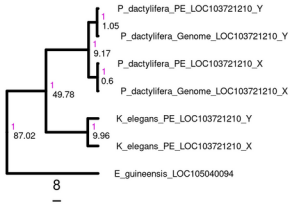
P_dactylifera_PE_LOC103721210_Y
P_dactylifera_Genome_LOC103721210_Y
P_dactylifera_PE_LOC103721210_X
P_dactylifera_Genome_LOC103721210_X
K_elegans_PE_LOC103721210_Y
K_elegans_PE_LOC103721210_X
E_guineensis_LOC105040094
1.05
9.17
0.6
49.78
87.02
9.96
8

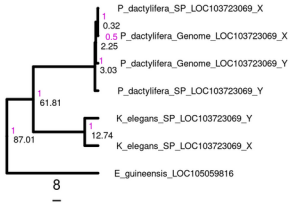
P_dactylifera_SP_LOC103723069_X
P_dactylifera_Genome_LOC103723069_X
P_dactylifera_Genome_LOC103723069_Y
P_dactylifera_SP_LOC103723069_Y
K_elegans_SP_LOC103723069_Y
K_elegans_SP_LOC103723069_X
E_guineensis_LOC105059816
0.32
0.5
2.25
3.03
61.81
87.01
12.74
8

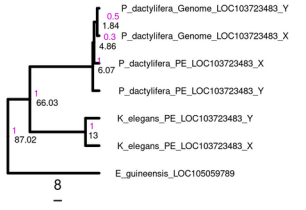
P_dactylifera_Genome_LOC103723483_Y
P_dactylifera_Genome_LOC103723483_X
P_dactylifera_PE_LOC103723483_X
P_dactylifera_PE_LOC103723483_Y
K_elegans_PE_LOC103723483_Y
K_elegans_PE_LOC103723483_X
E_guineensis_LOC105059789
0.5
1.84
0.3
4.86
6.07
66.03
87.02
13
8

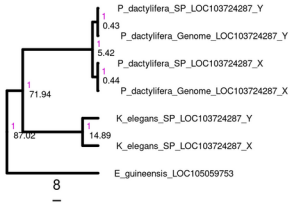
P_dactylifera_SP_LOC103724287_Y
P_dactylifera_Genome_LOC103724287_Y
P_dactylifera_SP_LOC103724287_X
P_dactylifera_Genome_LOC103724287_X
K_elegans_SP_LOC103724287_Y
K_elegans_SP_LOC103724287_X
E_guineensis_LOC105059753
0.43
5.42
0.44
71.94
87.02
14.89
8

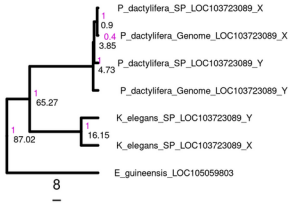
P_dactylifera_SP_LOC103723089_X
P_dactylifera_Genome_LOC103723089_X
P_dactylifera_SP_LOC103723089_Y
P_dactylifera_Genome_LOC103723089_Y
K_elegans_SP_LOC103723089_Y
K_elegans_SP_LOC103723089_X
E_guineensis_LOC105059803
0.9
0.4
3.85
4.73
65.27
87.02
16.15
8

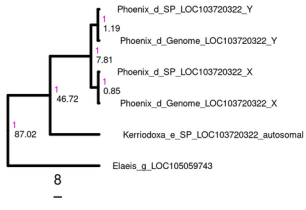
Phoenix_d_SP_LOC103720322_Y
Phoenix_d_Genome_LOC103720322_Y
Phoenix_d_SP_LOC103720322_X
Phoenix_d_Genome_LOC103720322_X
Kerriodoxa_e_SP_LOC103720322_autosomal
Elaeis_g_LOC105059743
1.19
7.81
0.85
46.72
87.02
8

53

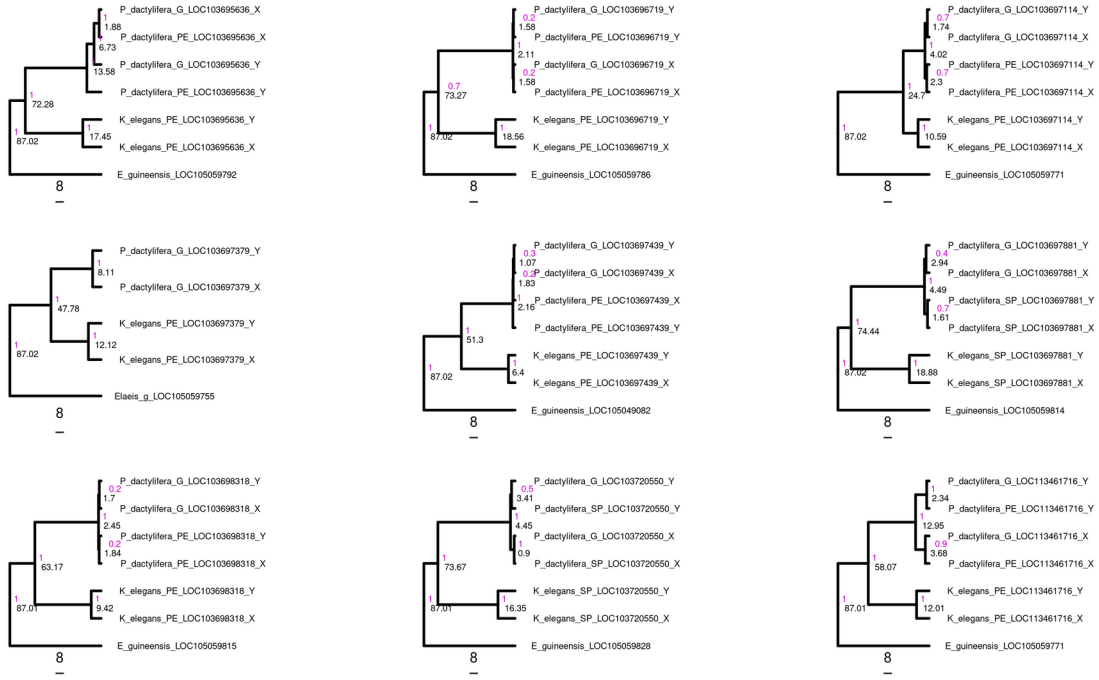

Figure S5. Phylogenies of sex-linked genes. Phylogenies of all sex-linked genes common to *K. elegans* and *P. dactylifera* (high-confidence sex-linked and probably sex-linked, File **S3**) and two known sex-linked genes in *P. dactylifera* : LOGlike (LOC103701078) and guanosine deaminase (LOC103720322). Two Y-specific sequences of *P. dactylifera* were taken from NCBI : GPAT3 (LOC120108105, MH668906), CYP703 (LOC120107104, MH668888). *Elaeis* guineensis root sequences were also taken from NCBI as the blastn top hit of *P. dactylifera* sequence. The node values are the posterior probabilities of the node colored in magenta and the mean age of the node in black. The scales below the trees are in million years.

54

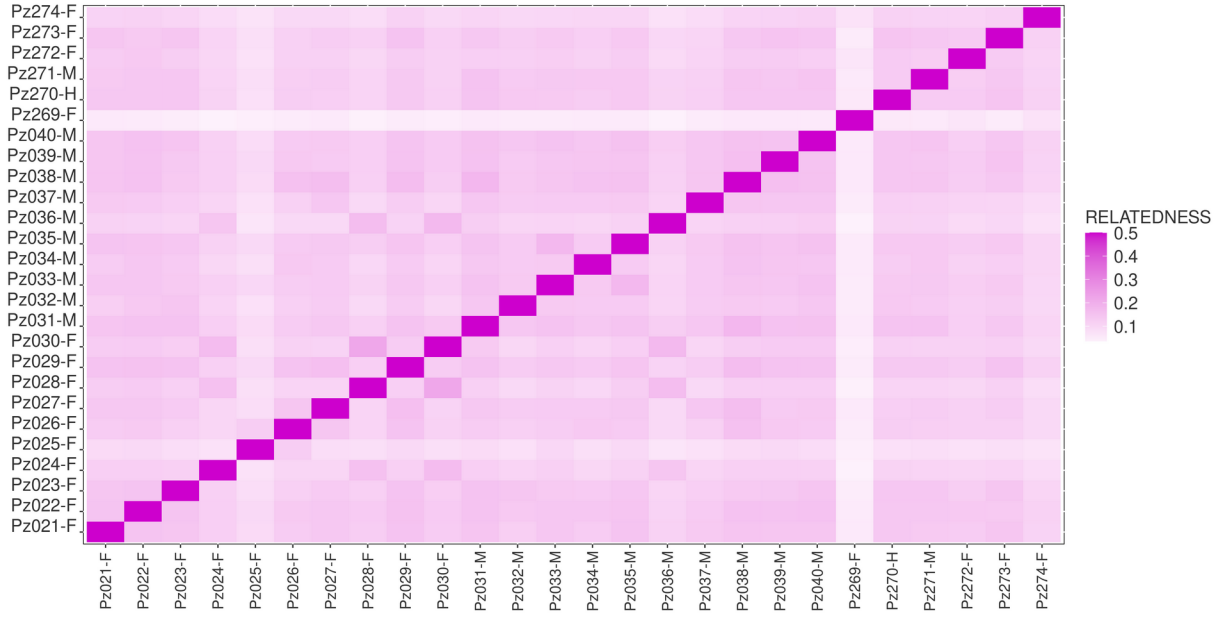

Figure S6. *Kerriodoxa elegans* heatmap of estimated relatedness with no paralogy bias. Genes with high posterior probabilities to be paralogous were removed from the data prior to estimating relatedness. A relatedness of 0 is represented by a white square and indicates unrelated individuals from the same population. A relatedness of 0.5 (the maximum value) is represented with a magenta square and is characteristic of clones. Gradients between white and magenta represent intermediate values.

55

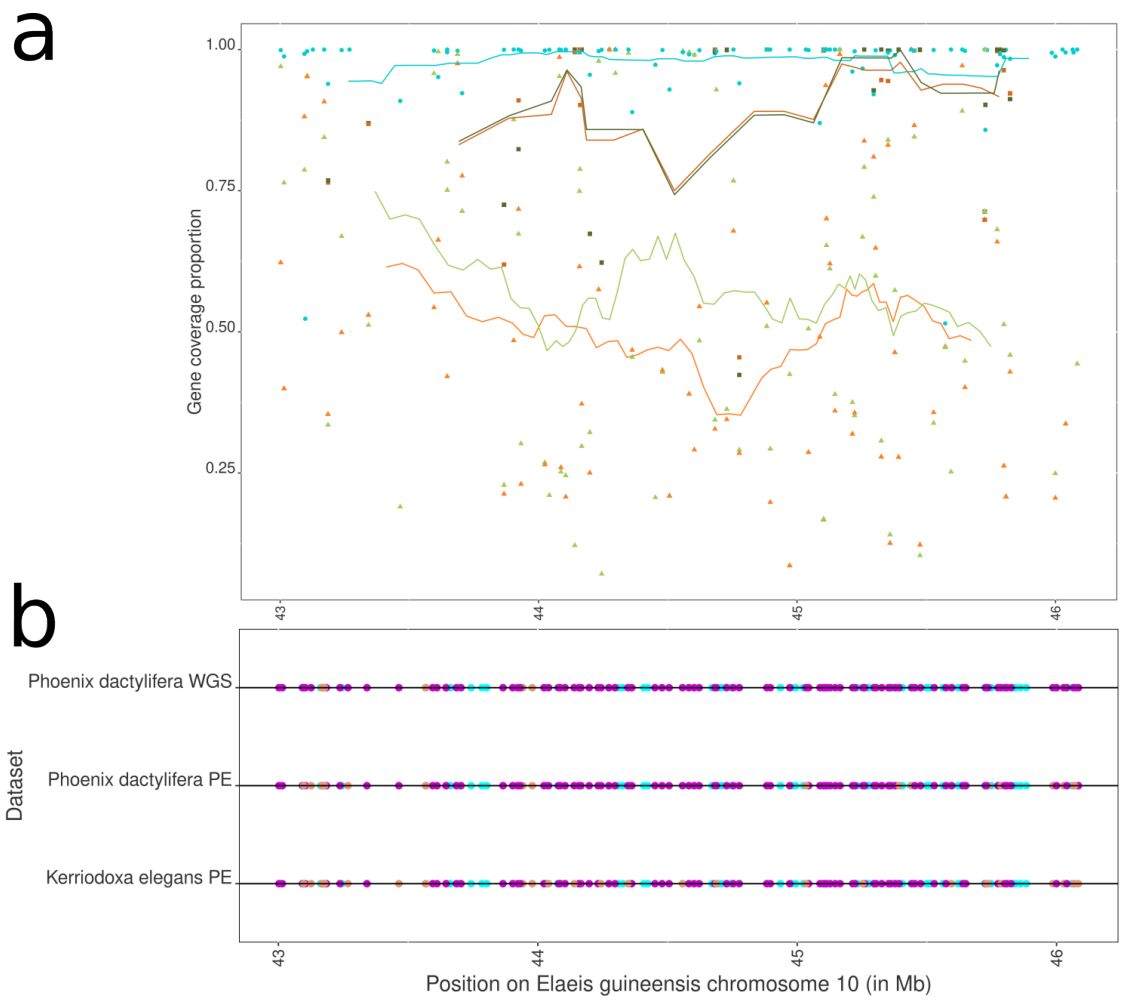

Figure S7: Sex-linked region coverage. (a) Proportion of each gene covered (as a fraction of the total length) with at least 7X depth for capture kits and 10X for whole genome sequencing (WGS) in the sex-linked region of *Phoenix dactylifera* and *Kerriodoxa elegans*, *using the corresponding region* on the *Elaeis guineensis* EGPMv6 genome as a reference. Each point represents a gene for the WGS (circle), the PalmExons sequence capture (triangle) and SexPhoenix sequence capture (square). They are colored in blue (WGS *Phoenix dactylifera*), green (sequence capture *P. dactylifera*), orange (sequence capture *Kerriodoxa elegans*) with lighter colors for PalmExons data and darker for SexPhoenix. **(b)** *P. dactylifera* DPV01 and *E. guineensis* EG5 genome annotations genes positioned via Liftoff on the *E. guineensis* EGPMv6 genome 10th chromosome between 43Mb and 46.1Mb. *P. dactylifera* genes are colored depending on their presence (magenta) or absence (lightpink) in a dataset (WGS or PE) and positions with genes unique to *E. guineensis* are colored in cyan.

56

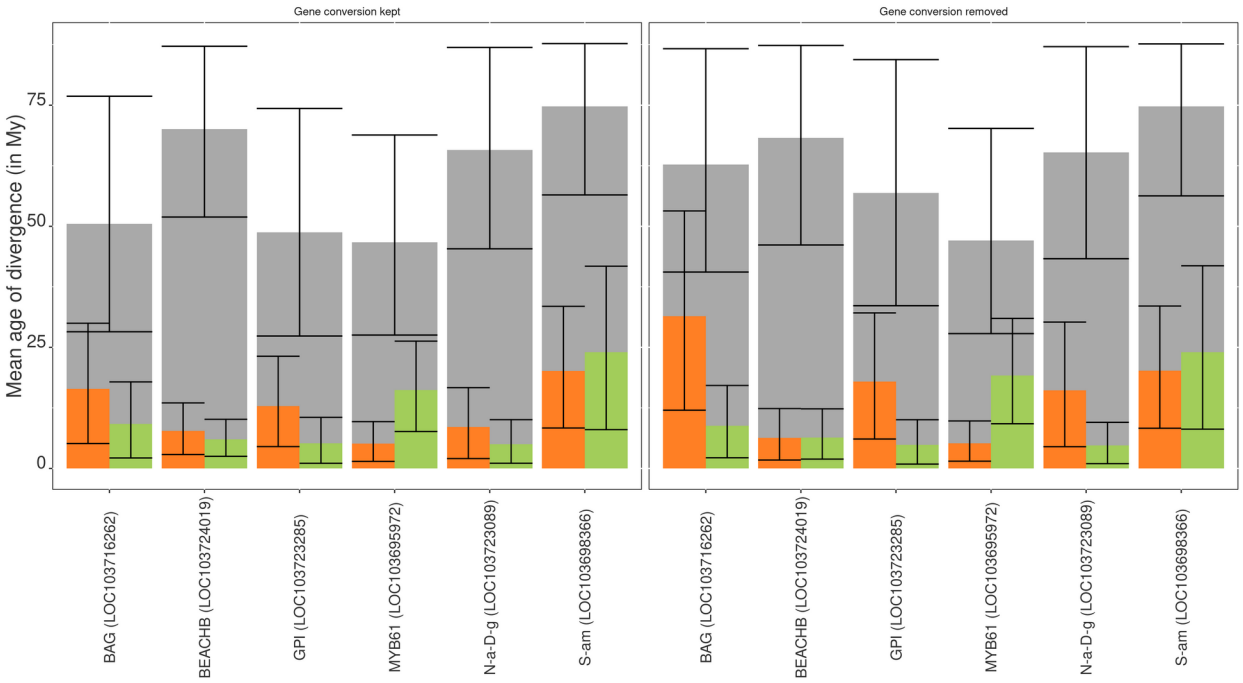

Figure S8. Effect of gene conversion between X and Y copies on node ages.

Mean age of divergence of X and Y sequences for common sex-linked genes with possible gene conversion. Gene fragments detected as having undergone gene conversion (see Table S8) were either retained in the analysis (left panel) or removed (right panel). *P. dactylifera* sex-linked sequence divergence estimates are colored in green, estimated for *K. elegans* in orange, and the estimates of the age of the split of the lineages between the two species in grey. Error bars correspond to the 95% probability density of the node age.

57

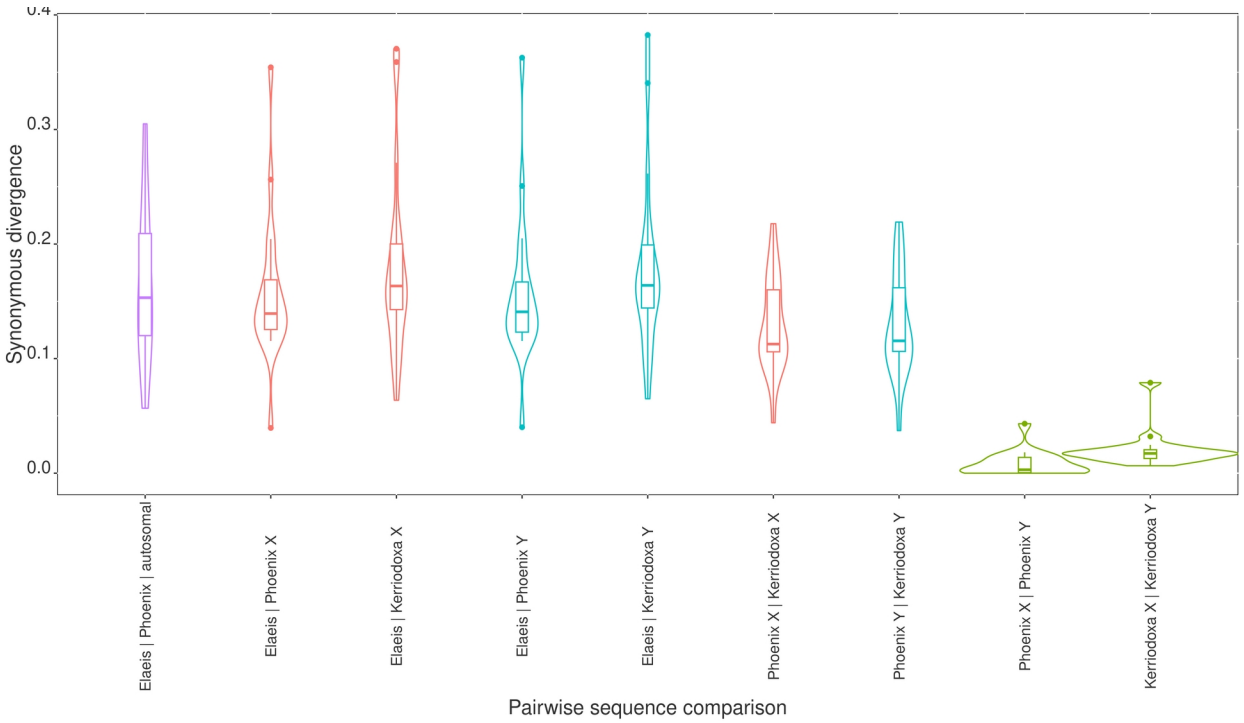

Figure S9. Synonymous divergence of sex-linked and autosomal nuclear genes. Violin plots and boxplots of the synonymous divergence (dS) of the 18 genes inferred as XY in SexPhoenix (SP) and 10 randomly selected autosomal single copy orthologs pertaining to the BUSCO *Liliopsidae* database. dS between X and Y sequences are colored in green, dS between X sequences from SP are colored in red, dS between Y sequences from SP are colored in cyan and dS between autosomal single copy orthologs are colored in purple.

58

File S1 (separate file). SexPhoenix target reference sequences available in EBI Project PRJEB76653.

File S2 (separate file). PalmExons baits sequences available in EBI Project PRJEB76653.

File S3. (separate file). Summary of all genes either inferred as XY in at least one dataset or aligned on the EGPMv6 genome (Ong *et al.*, 2020) on chromosome 10 between 43Mb and 46.1Mb. Each gene identification and annotation is documented as well as their position on the PDMBC4 genome (Hazzouri *et al.*, 2019), EG5 annotation (Singh *et al.*, 2013) and EGPMv6 (Ong *et al.*, 2020). This table contains the mean female and male depth per base as well as the mean female reads ratio, the number of polymorphisms and mean number of individual genotyped per polymorphism as well as the autosomal and XY posterior probability of each of these genes.

File S4. (separate file). Summary of all genes inferred as X-hemizygous in at least one dataset. Each sheet contains the X-hemizygous genes of one dataset. Since no X-hemizygous genes were found in any SexPhoenix dataset, no sheet is present in the file for these datasets. Each gene identification and annotation is documented as well as their position on the PDMBC4 genome (Hazzouri *et al.*, 2019), EG5 annotation (Singh *et al.*, 2013) and EGPMv6 (Ong *et al.*, 2020). This table contains the mean female and male depth per base as well as the mean female reads ratio, the number of polymorphisms and mean number of individual genotyped per polymorphism as well as the X-hemizygous posterior probability of each of these genes.

File S5. (separate file). GO annotation of the DPV01 P. dactylifera genome. Merged GO annotation of the DPV01 genome through the fantasia deep-learning method with the PDMBC4 P. dactylifera genome GO annotation of genes common to both assemblies' annotations. Each gene identification is referenced with the GO ID of the annotated GO terms for said gene.

File S6. (separate file). GO enrichment of the common sex-linked region: *Elaeis guineensis* EGPMv6 genome (Ong et al., 2020) chromosome 10, 43.3Mb to 46.1Mb. Enriched GO-IDs and terms are summarised. The number of genes annotated for each GO-id in the universe, the number present in the region of interest as well as the expected number are referenced with the estimated p-value of enrichment and the reference universe. SDpop-1X and SDpop-7X are the two gene universes used and are the list of genes present in the SDpop analysis with a respective mean depth per base of 1 and 7.

59